Mechanical formalism for tissue dynamics

Sham Tlili, Cyprien Gay, Francois Graner, Philippe Marcq, François Molino, Pierre Saramito

Mechanical formalism for tissue dynamics

Sham Tlili[1], Cyprien Gay[1,6], François Graner[1,6], Philippe Marcq[2], François Molino[3,4,6], and Pierre Saramito[5,6]
(1). Laboratoire Matière et Systèmes Complexes, Université Paris Diderot, CNRS UMR 7057, 10 rue Alice Domon et Léonie Duquet, F-75205 Paris Cedex 13, France
(2). Laboratoire Physico-Chimie Curie, Institut Curie, Université Marie et Pierre Curie, CNRS UMR 168, 26 rue d'Ulm, F-75248 Paris Cedex 05, France
(3). Laboratoire Charles Coulomb, UMR 5221 Univ. Montpellier II and CNRS, Place Eugène Bataillon, CC070, F-34095 Montpellier Cedex 5, France
(4). Institut de Génomique Fonctionnelle, CNRS UMR 5203, INSERM UMR_S 661, Univ. Montpellier I, Univ. Montpellier II, 141 rue de la Cardonille, F-34094 Montpellier cedex 05, France
(5). Laboratoire Jean Kuntzmann, UMR 5524 Univ. J. Fourier - Grenoble I and CNRS, BP 53, F-38041 Grenoble cedex, France and
(6). Academy of Bradylogists
(Dated: 27 Sept. 2013)

The understanding of morphogenesis in living organisms has been renewed by tremendous progress in experimental techniques that provide access to cell-scale, quantitative information both on the shapes of cells within tissues and on the genes being expressed. This information suggests that our understanding of the respective contributions of gene expression and mechanics, and of their crucial entanglement, will soon leap forward. Biomechanics increasingly benefits from models, which assist the design and interpretation of experiments, point out the main ingredients and assumptions, and can ultimately lead to predictions. The newly accessible local information thus urges for a reflection on how to select suitable classes of mechanical models. We review both mechanical ingredients suggested by the current knowledge of tissue behaviour, and modelling methods that can help generate a constitutive equation. We also recall the mathematical framework developped for continuum materials and how to transform a constitutive equation into a system of partial differential equations amenable to numerical resolution. The present article thus groups together mechanical elements and theoretical methods that are ready to enhance the significance of the data extracted from recent or future high throughput biomechanical experiments.

PACS numbers: 87.19.R- Mechanical and electrical properties of tissues and organs 87.19.lx Development and growth 83.10.Gr Constitutive relations 83.60.La Viscoplasticity; yield stress

I. INTRODUCTION

A. Motivations

Models based on either analytical equations or numerical simulations play several roles in biomechanics. They assist experiments to integrate and manipulate quantitative data, and extract measurements of relevant parameters (either directly, of through fits of models to data). They also help in proposing and designing new experiments, test the effect of parameters, simulate several realisations of a stochastic phenomenon, or simulate experiments which cannot be implemented in practice. They enable to illustrate an experiment, favor its interpretation and understanding. They point out the main ingredients and assumptions, test the sensitivity of an experiment to a parameter or to errors, and determine which assumptions are sufficient to describe an experimental result. Finally, models can help determining a causal relationship between two facts, and also lead to predictions.

The pioneering work of XIXth century biologists and physicists initiated the mechanical modelling of animal tissues, now an important field of study. Two themes have dominated the recent literature: *(i)* modelling the mechanics of some specific adult tissues like bones or muscles, for which deformations and stresses are obviously part of the biological function [1]; and *(ii)* unraveling the role of forces in the generation of forms during embryonic development [2, 3]. During the last decades, both the physics and the biology sides of the problem have been completely transformed, especially by progress in imaging.

On the physics side, new materials with complex structures (namely *complex fluids*) have been thoroughly studied, especially in the last twenty years, with a strong emphasis on the difficult problem of the feedback between the microscopic structure and the mechanical response [4]. The development of new tools to image the changes in the cell arrangement under well-controlled global stresses or deformations has provided a wealth of data. Modelling has played a crucial part *v*ia the determination of so-called constitutive equations. A constitutive equation characterises the local properties of a material within the framework of continuum mechanics. It relates dynamical quantities, such as the stress carried by the material, with the kinematical quantities, *e.g.* the deformation (also called "strain") or the deformation rate.

On the biology side, analogous questions now arise regarding the interplay of cell scale behaviour and tissue scale mechanical properties.

A first question is how a collective behaviour not obviously apparent at the cell scale emerges at the tissue scale. Analyses of images and movies lead to the conclusion that epithelia or whole embryos behave like *viscous liquids* on long time scales [5]. The physical origin and the value of the (effective) viscosity should be traced back to the cell dynamics: it can in principle incorporate contributions from ingredients such as cell divisions and apoptoses [6] or cell contour fluctuations [7], but also from orientational order, cell contractility, cell motility or cell rheological properties. All these local and sometimes changing ingredients become progressively accessible to experimental measurements. Biomechanical models can investigate the bottom-up relationship between local cell-scale structure and tissue-scale mechanical behaviour, unraveling the signature of the cellular structure in the continuum mechanics descriptions.

Conversely, a second question is how the mechanical state of the tissue may have an influence on the cell division rate [8, 9], or on the orientation of the cells undergoing division [10]. In addition, the mechanical state of the tissue can generate cell polarity and hence an anisotropy of the local cell packing, which may affect the mutual influence between the local mechanics (forces and deformations) and the cell behaviour. Biomechanical models contribute to disentangle these complex feedback loops and address such top-down relationships.

To address this type of questions, a natural strategy is first to reconstruct the mechanics from the structural description, then to investigate the feedback between well-identified mechanical variables and the expression of specific genes. In particular, this interplay between genes and mechanics is expected to be the key to the spontaneous construction of the adult form in a developing tissue without an organising center. Such problem in its full complexity will probably require a "systems biology" approach. Large scale mapping of expression for at least tens of genes, coupled to a correct mechanical modelling on an extended range of scales in time and space will be necessary, which in turn supposes experimental setups able to produce the relevant genetic and mechanical data.

B. State of the art

Recent developments in *in vivo* microscopy now give access to the same richness of structural information for living tissues as for complex fluids. The biology of cells and tissues is now investigated in detail in terms of protein distribution and gene expression, especially during development [11]. It is possible to image the full geometry of an embryonic tissue at cellular resolution [12, 13], while simultaneously visualising the expression of various genes of interest [14–16]. Mechanical fields such as the deformation, deformation rate or plastic deformation rate are increasingly accessible to direct measurement. Several fields can be measured quantitatively at least up to an unknown prefactor. This is the case for *(i)* some protein distributions, *via* quantitative fluorescence [17]; *(ii)* elastic forces and stresses, either by laser ablation of cell junctions [18] and tissue domains [19], or through image-based force inference methods based on images [20–23]; *(iii)* even viscous stress fields, indirectly estimated [16]. Preliminary experiments include absolute measurements of forces based on micro-manipulation, *in situ* incorporation of deformable force sensors, or fluorescence resonance energy transfer (FRET).

In vitro assemblies of cohesive cells are useful experimental systems. Within a reconstructed cell assembly, each individual cell retains its normal physiological behaviour: it can grow, divide, die, migrate, etc. In the absence of any regulatory physiological context, cells display small or negligible variation of gene expression. Reconstructed systems thus allow to separate the mechanical behaviour of a tissue from its feedback to and from genetics. Further, in absence of any coordinated variation of the genetic identity of constituent cells, spatial homogeneity may be achieved. Simple, well-controlled boundary conditions can be implemented by a careful choice of the geometry, either in two or three dimensions.

In two dimensions, confluent monolayers are usually grown on a substrate used both as a source of external friction and as a mechanical sensor to measure local forces [24–26]. 2D monolayers make easier experiments, simulations, theory and their mutual comparisons [27–30]. 2D images are easier to obtain and can be analysed in detail; data are more easily manipulated, both formally and computationally.

In three dimensions, multi-cellular spheroids in a well-controlled, *in vitro* setting [7, 8, 31] are a good model system to mimic the mechanical properties of tumors, and of homogeneous parts of whole organs, either adult or during development. They are also useful for rheological studies [32, 33], especially since they are free from contact with a solid substrate. Although the full reconstruction of the geometry of multi-cellular spheroids at cellular resolution remains challenging, progress is fast [34].

C. Outline of the paper

A tissue can be seen as an amorphous cellular material that is *active*, in the sense that it is out of equilibrium thanks to its reservoir of chemical energy; a consequence of this activity being its ability to autonomously generate forces, as well as motion. We compare three main formalisms used to construct constitutive equations indifferently in 2D or 3D for such active materials: *(i) rheological diagrams*; *(ii) linear out-of-equilibrium thermodynamics*, also called "hydrodynamics"; and *(iii) the dissipation function* formalism, for so-called "generalised standard materials". We would like here to guide the choice of models according to the tissue under consideration, the experimental set-up, the scientific question

raised and the search for simplicity. We propose a framework for the analysis of experimental data (movies) with a fully tensorial treatment of spatially heterogeneous tissues. Although the simplest applications concern *in vitro* experiments, often performed with epithelial cells, the same approach applies to a wide spectrum of living tissues.

This article is organised as follows. Section II makes explicit our assumptions and arguments to choose a formalism. Section III reviews mechanical ingredients suitable for the theoretical description of a wide range of living tissues, both *in vitro* and *in vivo*, with worked out examples. Section IV summarizes and opens perspectives.

II. CHOICES AND METHODS

In this Section, we explain our choices and our assumptions. Section II A compares discrete and continuum approaches. Section II B compares rheological diagrams, hydrodynamics, and the dissipation function formalisms. Section II C explains why an Eulerian description is appropriate for developing tissues. Section II D suggests how to incorporate space dependence in constitutive equations to write partial differential equations.

A. A continuum rather than a discrete description

Models that describe tissue mechanical properties may be broadly split into two main categories: discrete "cell-based" simulations (Section II A 1) and continuum mechanics models (Section II A 2). We explain why we favor here the latter (Section II A 3).

1. Discrete models

Direct cellular simulations build upon the (supposedly known) geometry and rheology of individual cells and membranes, and generate global tissue behaviour through the computation of the large-scale dynamics of assemblies of idealised cells [35–42]. Simulations enable to directly test the collective effect of each cell-scale ingredient, and of their mutual feedbacks. Also, they work well even for a small number of cells, where the length scale of a single cell and that of the cell assembly are comparable.

2. Continuum models

A continuum approach requires the existence of an intermediate length scale, larger than a typical cell size, yet smaller than the tissue spatial extension, and beyond which the relevant fields vary smoothly. The continuum rheology is captured through a constitutive equation relating the (tensorial) stresses and deformations [43–49]. This rheological model is incorporated into the usual framework of continuum mechanics using fundamental principles such as material and momentum conservation. When it succeeds, a continuum approach yields a synthetic grasp of the relevant mechanical variables on an intermediate scale (*i.e.* averaged over many individual cells), and helps dealing with large systems. It often involves a smaller number of independent parameters than a discrete approach, which helps comparing with experimental observations. Note that continuum models have also been applied to vegetal tissues, as in plant growth [50].

In order to test and calibrate a continuum model, it is generally necessary to extract continuum information from other sources such as discrete simulations or experiments on tissues with cell-scale resolution. Powerful tools, described in Appendix A, have been developed in recent years to process segmented experimental movies in order to extract tensorial quantities such as the elastic deformation rate and the plastic deformation rate.

3. Choosing continuum models

In the following, we choose to concentrate on continuum models, drawing inspiration from both models of (non-living) amorphous cellular materials such as liquid foams [51] or emulsions [52], and from models of living matter that incorporate ingredients such as cell division [6] and orientational order [48, 49].

The continuum models describing amorphous cellular materials can be tensorial and incorporate viscoelastoplastic (VEP) behaviour [47, 53–56]. In addition to the viscous and elastic behaviour expected for a complex fluid whose microstructure can store elastic deformation, one incorporates the ingredient of plasticity capturing irreversible structural changes, more specifically here local reorganisations of the individual cells due to relative motion and neighbour exchange, or even plasticity within the cells. A VEP model assembling these ingredients, with additional ones pertaining to living cells, could capture the different "short-time" phenomena described in Section III and at the same time display a viscous liquid-like behaviour on longer time scales.

B. Choice of the dissipation function formalism

In this Section, we discuss three general formalisms used to construct constitutive equations (indifferently in 2 or 3D): rheological diagrams (Section II B 1), hydrodynamics in its general sense (Section II B 2) and the dissipation function method (Section II B 3).

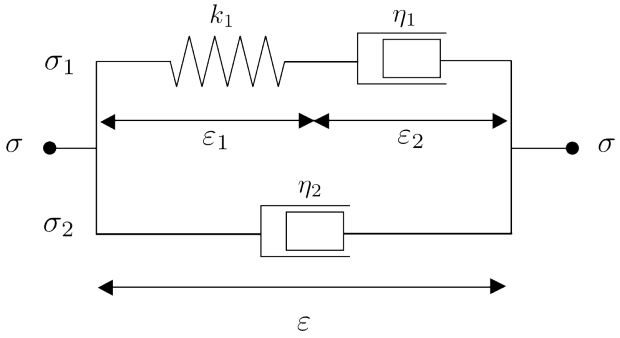

FIG. 1: An example of a rheological diagram: a dashpot with viscosity η_2 in parallel with a Maxwell element (spring with stiffness k_1 in series with a dashpot with viscosity η_1).

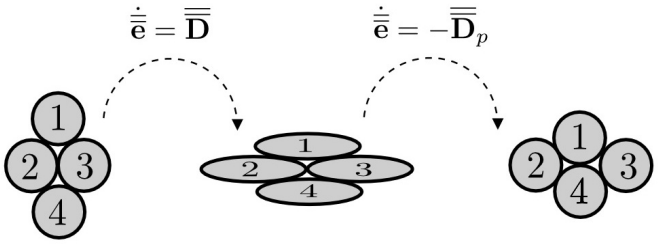

FIG. 2: Cell rearrangement. Cells 2 and 3 are initially in contact (left). Cells deform (center) and can reach a configuration with a new topology where cells 1 and 4 are now in contact (right). See Eq. (20) for notations $\overline{\overline{\mathbf{D}}}$, $\dot{\overline{\overline{\mathbf{e}}}}$ and $\overline{\overline{\mathbf{D}}}_p$, which refer to the continuum description: upon coarse-graining at the tissue scale, the discontinuities at the cell scale are wiped out.

1. *Rheological diagram formalism*

Let us consider the rheological diagram of Fig. 1: it represents the well-known viscoelastic Oldroyd fluid model. It consists in a dashpot with viscosity η_2 and deformation ε carrying the stress σ_2 in parallel with a Maxwell element carrying the stress σ_1. This Maxwell element is itself made of a spring (stiffness k_1, deformation ε_1) in series with a dashpot (viscosity η_1, deformation ε_2). The elementary rheological equations read:

$$\varepsilon = \varepsilon_1 + \varepsilon_2 \tag{1}$$
$$\sigma = \sigma_1 + \sigma_2 \tag{2}$$
$$\sigma_2 = \eta_2 \, \dot{\varepsilon} \tag{3}$$
$$\sigma_1 = k_1 \, \varepsilon_1 \tag{4}$$
$$\sigma_1 = \eta_1 \, \dot{\varepsilon}_2 \tag{5}$$

Eliminating ε_1, $\dot{\varepsilon}_1$, ε_2 and $\dot{\varepsilon}_2$ between these equations yields:

$$\dot{\sigma} + \frac{k_1}{\eta_1} \, \sigma = \frac{\eta_1 + \eta_2}{\eta_1} \, k_1 \, \dot{\varepsilon} + \eta_2 \, \ddot{\varepsilon} \tag{6}$$

Such a straightforward method is useful when physical knowledge or intuition of the mechanical system is sufficient to determine the topology (nodes and links) of the diagram. Note that the relationship between a rheological diagram (such as that presented by Fig. 1) and a constitutive equation (such as Eq. (6)) is *not* one-to-one: see Appendix B for an example.

2. *Hydrodynamic formalism*

When non-mechanical variables are present, the rheological diagram formalism (Section II B 1) is not sufficient to establish the constitutive equation. Another formalism is necessary to include couplings between mechanical and non-mechanical variables. A possible formalism is linear out-of-equilibrium thermodynamics, also called "hydrodynamics" [57] although its range of application is much larger than the mechanics of simple fluids.

Broadly speaking, hydrodynamics may be defined as the description of condensed states of matter on slow time scales and at large length scales. Macroscopic behaviour is characterized by the dynamics of a small number of slow fields (so-called "hydrodynamic fields"), related to conservation laws and broken symmetries [57]. On time scales long compared to the fast relaxation times of microscopic variables, the assumption of local thermodynamic equilibrium leads to the definition of a thermodynamic potential as a function of all relevant (long-lived) thermodynamic variables and their conjugate quantities. Standard manipulations lead to the expression of the entropy creation rate as a bilinear functional of generalized fluxes and forces. In the vicinity of equilibrium, generalized fluxes are expressed as linear combinations of generalized forces, where cross-coefficients are equal due to Onsager symmetry theorem [58].

The hydrodynamic formalism is physically intuitive. It is flexible and can accommodate a broad spectrum of physical quantities, as long as deviations from equilibrium can be linearised. The approach is quite general since it relies on thermodynamic principles and on the invariance properties of the system. Constitutive equations may thus be written within the domain of linear response as linear relationships between generalized fluxes and forces. This approach has been highly successful, leading for instance to the derivation of the hydrodynamics of nematic liquid crystals (with the nematic director field as an additional, non-conserved hydrodynamic variable) [59, 60], or, more recently, of soft active matter (where a chemical field typically couples to an orientational order parameter to model, *e.g.* cytoskeletal mechanics) [61].

3. Dissipation function formalism

Not all materials are linear. In tissues, plastic events such as cell rearrangements [14], see Fig. 2, have thresholds which break down the linearity, and hydrodynamics becomes inadequate (Section II B 2). Deriving constitutive equations requires a more general formalism.

In the dissipation function formalism, the state of the system is described by the total deformation ε and by $m \geq 0$ additional, independent, internal variables ε_k, with $1 \leq k \leq m$. These variables may be scalar, polar, axial or tensorial (see Appendix C). So-called "generalized standard materials" are defined by the existence of the free energy function $\mathcal{E}$ and the dissipation function $\mathcal{D}$ [62–64], which are convex functions of their respective arguments:

$$\mathcal{E} = \mathcal{E}(\varepsilon, \varepsilon_1, \ldots, \varepsilon_m) \quad (7)$$

$$\mathcal{D} = \mathcal{D}(\dot{\varepsilon}, \dot{\varepsilon}_1, \ldots, \dot{\varepsilon}_m) \quad (8)$$

Here $\dot{\varepsilon}$ denotes the total rate of deformation and $\dot{\varepsilon}_k = (\partial_t + \vec{v} \cdot \nabla)\varepsilon_k$ the Lagrangian time derivative of ε_k.

The dissipation function $\mathcal{D}$ is not the rate of entropy production: it is an integral of the movement (like a stream function in two-dimensional fluid mechanics, or a vector potential in electro-magnetism), defined up to an additive constant. It must be continuous and convex, but does not need to be differentiable. The convexity warrants that the model satisfies the second principle of thermodynamics [62, 65]. Numerically, it allows to use a variational approach, which makes it very useful for the resolution of the dynamical equations [66, 67]. Constitutive and evolution equations are obtained through the following rules:

$$\sigma = \frac{\partial \mathcal{D}}{\partial \dot{\varepsilon}} + \frac{\partial \mathcal{E}}{\partial \varepsilon} \quad (9)$$

$$0 = \frac{\partial \mathcal{D}}{\partial \dot{\varepsilon}_k} + \frac{\partial \mathcal{E}}{\partial \varepsilon_k}, \ 1 \leq k \leq m \quad (10)$$

where σ denotes the stress.

The dissipation function formalism is suitable for non-linear terms. For a given variable ε_k, quadratic terms ε_k^2 in the energy function or $\dot{\varepsilon}_k^2$ in the dissipation function are harmonic, *i.e.* they yield a linear term ε_k or $\dot{\varepsilon}_k$ in the derived dynamical equations, exactly like in the hydrodynamics formalism (Section II B 2). Terms of the form $|\varepsilon_k|^n$ or $|\dot{\varepsilon}_k|^n$, with $n \geq 1$ (n integer or real) yield non-linear terms $|\varepsilon_k|^{n-2}\varepsilon_k$ or $|\dot{\varepsilon}_k|^{n-2}\dot{\varepsilon}_k$ in the dynamical equations. Interestingly, the dissipation function can even treat the particular case $n = 1$ which corresponds to terms like $|\varepsilon_k|$ or $|\dot{\varepsilon}_k|$. This yields terms of the form $\varepsilon_k/|\varepsilon_k|$ or $\dot{\varepsilon}_k/|\dot{\varepsilon}_k|$ in the derived equations: these are non-linear terms which dominate over the linear ones. This lowest-order case is particularly important when we want to include plasticity (see Section III A for an example), whose treatment thus becomes straightforward [62, 64]. As a result, the dissipation function formalism has been successfully applied to viscoelastoplastic flows in [68, 69].

For purely mechanical systems made of springs, dashpots and sliders, the dissipation function formalism is by construction equivalent to directly writing the dynamical equations from the rheological model. For instance, the system discussed in Section II B 1 can be described within the formalism of Eqs. (7-10) with $m = 1$:

$$\mathcal{E}(\varepsilon, \varepsilon_1) = \frac{1}{2}k_1\varepsilon_1^2 \quad (11)$$

$$\mathcal{D}(\dot{\varepsilon}, \dot{\varepsilon}_1) = \frac{1}{2}\eta_1(\dot{\varepsilon} - \dot{\varepsilon}_1)^2 + \frac{1}{2}\eta_2\dot{\varepsilon}^2 \quad (12)$$

$$\sigma = \eta_1(\dot{\varepsilon} - \dot{\varepsilon}_1) + \eta_2\dot{\varepsilon} \quad (13)$$

$$0 = k_1\varepsilon_1 + \eta_1(\dot{\varepsilon}_1 - \dot{\varepsilon}) \quad (14)$$

Eliminating ε_1 and $\dot{\varepsilon}_1$ between Eqs. (13) and (14) indeed yields Eq. (6).

For systems with non-mechanical ingredients, the dissipation function formalism allows to systematically explore possible couplings (see Section III D for examples). The coupling coefficients arise as cross partial derivatives, with the advantage that they derive from a smaller number of free parameters than in the hydrodynamics formalism. A second advantage is that they automatically obey the Onsager symmetry [58]. In view of these advantages, and since it allows to treat plasticity, we recommend to adopt the dissipation formalism for living tissues.

C. An Eulerian rather than a Lagrangian approach

We now compare the Lagrangian and Eulerian points of view, and explain why we choose the latter.

1. Main variable associated with each approach

For materials that retain information about their initial state, it is natural (and common) to use a deformation variable (usually ε) that compares the current local material state to the initial state of the same material region. This is called the Lagrangian description and is usually preferred for elastic solids.

By contrast, in materials that have no or little memory of past configurations, such as viscous or viscoelastic fluids, it is common practice to use only the current velocity field $\vec{v}(\vec{x}, t)$ as the main variable, with no reference to any initial state. This is called the Eulerian description, used for instance when writing the Navier-Stokes equations.

2. Link between Lagrangian and Eulerian approaches

The deformation ε of the Lagrangian approach and the velocity field $\vec{v}(\vec{x}, t)$ of the Eulerian point of view are tightly connected. Indeed, the Lagrangian time derivative of the deformation is equal to (the symmetric part of) the velocity gradient. This quantity is also called

deformation rate and can be expressed in one and more spatial dimensions respectively as:

$$\dot{\varepsilon} = \left(\frac{\partial}{\partial t} + v\frac{\partial}{\partial x}\right)\varepsilon = \frac{\partial v}{\partial x} \quad (15)$$

$$\dot{\bar{\bar{\varepsilon}}} = \left(\frac{\partial}{\partial t} + \vec{v}\cdot\nabla\right)\bar{\bar{\varepsilon}} = \frac{\nabla\vec{v} + \nabla\vec{v}^T}{2} = \bar{\bar{\mathbf{D}}} \quad (16)$$

where we have introduced the notation $\bar{\bar{\mathbf{D}}}$ for the deformation rate tensor.

3. Choosing the Eulerian point of view

In materials such as developing tissues, the plastic flow, that results in particular from cell rearrangements or divisions, progressively erases the memory of the initial material configuration (this is similar to the role played by bubbles or droplets rearrangements in liquid foams or emulsions, respectively). Therefore, once the sample has been deformed substantially, the *total* deformation ε with respect to the initial state loses its physical relevance. Moreover, it is no longer a useful variable for the numerical resolution of evolution equations.

By contrast, the Eulerian point of view is relevant not only for common fluids, but also in the case of cellular materials, as discussed in detail in Ref. [53]. Fortunately, the current material state and evolution can be quantified without any reference to earlier configurations using tools for image and film analysis (Appendix A). This enables to analyse experiments within the Eulerian point of view. Therefore, we recommend to adopt the Eulerian viewpoint for developing tissues.

Moreover, these tools provide access to the *elastic* deformation e, defined as the deformation which can be recovered upon release of the stress (through local ablation for example [18, 19], see Appendix D for a precise definition). The elastic deformation e is the only part of the total deformation ε that remains relevant in the Eulerian context.

4. Notations for dissipation function formalism

To use the Eulerian point of view requires to express the constitutive equations only in terms of physically meaningful variables. We should thus only keep the elastic deformation e equal to, say, ε_1. All other deformation variables ε or ε_k should not play any role, and only their deformation rates $\bar{\bar{\mathbf{D}}}$ and $\bar{\bar{\mathbf{D}}}_k = \dot{\varepsilon}_k$ should be included in the final equation.

Yet in the dissipation function formalism, constitutive equations (Eqs. (9,10)) are explicitely expressed in terms of the deformation variables ε_k. How can this be compatible with the Eulerian point of view?

In fact, in the case of a fluid material, it is always possible to eliminate all irrelevant deformation variables from Eqs. (9,10). An example has been provided in Section II B 3: Eqs. (13,14) still contain ε_1, which is the elastic deformation of the spring on Fig. 1, but they do not contain ε. Note that they can be combined into Eq. (6), which is furthermore free of ε_1. Similarly, for each example discussed in Section III below, we initially use deformation variables ε_k to construct the energy and dissipation functions. We then formally replace the deformation rate variables $\dot{\varepsilon}_k$ with more intuitive notations, such as g for the growth rate or $\bar{\bar{\mathbf{D}}}_p$ for the plastic deformation rate. Eventually, equations are combined to naturally eliminate all ε_k variables, except the elastic deformation $e = \varepsilon_1$ of the material and possibly other deformation variables that are relevant in the Eulerian framework.

D. System of partial differential equations

A tissue may be spatially heterogeneous: its material properties, its history, its interaction with its environment may depend on the position $\vec{x}$. For instance the tissue may comprise different cell types or it may be placed on a spatially modulated substrate. The parameters and variables which describe the tissue are fields that may vary spatially. For simplicity we here assume that they are continuous and differentiable. The evolution of the entire system is then expressed as a set of partial differential equations (PDE), consisting in conservations laws and constitutive equations.

To make this article self-contained, we show in this Section how constitutive relations, such as derived using the dissipation function formalism, can be embedded in the rigorous framework of continuum mechanics in order to obtain a closed system of evolution equations. In continuum mechanics, one usually starts from the conservation equations of mass, momentum and angular momentum. The mass conservation equation reads:

$$\frac{\partial\rho}{\partial t} + \nabla\cdot(\rho\vec{v}) = s \quad (17)$$

where ρ is the mass density (or mass per unit area in 2D); and s represents material sources or sinks which, in the context of a tissue, can be cell division and apoptosis, respectively. In general, the conservation of momentum reads:

$$\rho\,\vec{a}(\vec{x},t) = \nabla\cdot\bar{\bar{\sigma}}(\vec{x},t) + \vec{f}(\vec{x},t) \quad (18)$$

which relates the acceleration $\vec{a} = \frac{\partial\vec{v}}{\partial t} + (\vec{v}\cdot\nabla)\vec{v}$ to the internal stress tensor $\bar{\bar{\sigma}}$ and the external forces $\vec{f}$. For instance, the external force $\vec{f}$ may contain a *friction* component $\vec{f} = -\zeta\vec{v}$ [19]. Note that, in a tissue, the inertial term $\rho\,\vec{a}$ is generally negligible when compared to the stress term $\nabla\cdot\bar{\bar{\sigma}}$. The validity of this approximation has to be checked in specific examples by estimating the value of the relevant dimensionless number, *e.g.* the Reynolds number for a purely viscous material, or the elastic num-

ber for a purely elastic solid.

Finally, the conservation of angular momentum implies that the stress tensor is symmetric [57]: $\sigma_{ij} = \sigma_{ji}$.

We obtain a set of $m + 4$ evolution equations (9,10,16,17,18). There are $m + 4$ unknown fields: σ, $(\varepsilon_k)_{1\leq k\leq m}$, $\dot{\varepsilon}$, ρ and $\vec{v}$. This system of partial differential equations is closed by suitable initial and boundary conditions. Its solution can be estimated by numerical resolution: see e.g. [54, 66, 67, 70, 71] for such numerical methods in the context of liquid foam flows.

In the case of large deformations, the Eulerian framework for time derivatives of tensorial quantities requires the use of objective derivatives [62, 72–74]. As shown in [53] and summarized in Appendix D, this leads to consider the upper-convected derivative, defined for any tensor $\overline{\overline{\mathbf{Q}}}$ by:

$$\frac{\partial\overline{\overline{\mathbf{Q}}}}{\partial t} + (\vec{v}\cdot\nabla)\,\overline{\overline{\mathbf{Q}}} - \nabla\vec{v}\,\overline{\overline{\mathbf{Q}}} - \overline{\overline{\mathbf{Q}}}\,\nabla\vec{v}^T \tag{19}$$

This is the only objective derivative that ensures that the dynamical equations respect the principle of covariance [75].

III. INGREDIENTS FOR TISSUE MODELLING

A (non-exhaustive) list of ingredients for tissue modelling includes viscosity, elasticity, plasticity, growth, chemical concentration fields, orientational order parameters, and their feedbacks. In this Section, we present worked out examples showing that each of these ingredients is easily taken into account within the dissipation function formalism, where the choice of a rheology and of a coupling scheme remains as simple as possible; it can be made more complex, along the same lines, if required, for a given tissue. In most cases, the energy and dissipation functions are written in reference to a given rheological model. Note that other tissue-specific ingredients, such as (possibly active) boundary conditions [76], do not contribute to constitutive equations themselves.

A. Plasticity

Recent experiments performed on cell aggregates and cell monolayers have shown that these tissues can have a yield stress [29, 33] and display a plastic behavior [7, 77]. The origin of this plasticity includes cell rearrangements [78, 79] (also known as : intercalation, neighbour swapping, or T1 process [14, 51]), which also play an important role during development, as in *e.g.* convergence-extension [11].

1. Rearrangements and plastic deformation rate

At the cell scale, and independently of its biological origin and regulation, a cell rearrangement (Fig. 2) is mathematically speaking a topological process, by which the rest state of a group of neighbour cells changes discontinuously. The associated mechanical description is decomposed into two steps. Before the rearrangement, the cells deform visco-elastically. After the rearrangement, they reach a new configuration, where two of the cells become closer while the two other cells move apart. The net result is an irreversible change in the rest state of the tissue, with convergence along one axis and extension along the perpendicular one. It is thus best described as a tensor with positive and negative eigenvalues [53, 80], called the plastic deformation rate $\overline{\overline{\mathbf{D}}}_p$ in the continuum limit (see also Appendix A). Semi-quantitatively, this tensor is related to the total deformation rate $\overline{\overline{\mathbf{D}}}$ and the elastic deformation rate $\dot{\overline{\mathbf{e}}}$:

$$\overline{\overline{\mathbf{D}}} \approx \dot{\overline{\mathbf{e}}} + \overline{\overline{\mathbf{D}}}_p \tag{20}$$

More precisely, using the transport of tensor $\overline{\mathbf{e}}$ by the velocity field provided by Eq. (D7), as shown in Appendix D, we obtain:

$$\dot{\overline{\mathbf{e}}} \;=\; \overline{\overline{\mathbf{D}}} + \nabla\vec{v}\,\overline{\mathbf{e}} + \overline{\mathbf{e}}\,\nabla\vec{v}^T - \overline{\overline{\mathbf{D}}}_p \tag{21}$$

where the fields $\vec{v}$, $\overline{\mathbf{e}}$, $\overline{\overline{\mathbf{D}}}$ and $\overline{\overline{\mathbf{D}}}_p$ depend on $(\vec{x}, t)$.

The plastic deformation rate $\overline{\overline{\mathbf{D}}}_p$ relaxes the tissue elastic deformation while usually leaving the volume unchanged. As seen in Appendix D 4, the volume conservation condition is:

$$\mathrm{Tr}\left[\left(\overline{\mathbf{I}} + 2\overline{\mathbf{e}}\right)^{-1}\overline{\overline{\mathbf{D}}}_p\right] = 0 \tag{22}$$

2. Example

Although plasticity is intrinsically tensorial, scalar models of rearrangements provide one dimensional analogies which help understand their effect on the mechanics of foams [81]. Inspired by Ref. [56], we now treat explicitly a 1D example that combines the (intracellular) rheology of the cell, considered here for simplicity as a viscoelastic solid, and the (intercellular) rheology of the tissue, considered here as viscoplastic (Fig. 3). Let us model the individual cells by a Voigt element with a dashpot representing the cytosplasm viscosity η_{cyto}, and a spring representing the cellular cortex elasticity K_{cortex}. It means that the cell cytoplasm behaves like a viscous fluid on short timescales but that the cell cortex can only be elastically deformed. Hence the cell as a whole (cytoplasm plus cortex) behaves like a viscoelastic solid. When the stress exerted on the tissue exceeds the yield stress σ_Y, the links between cells start to break and the cells

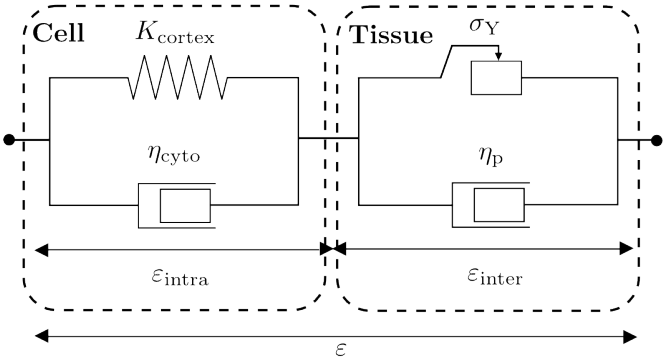

FIG. 3: Rheological diagram for a viscoelastoplastic model. The intracellular rheology is viscoelastic, the intercellular one is viscoplastic.

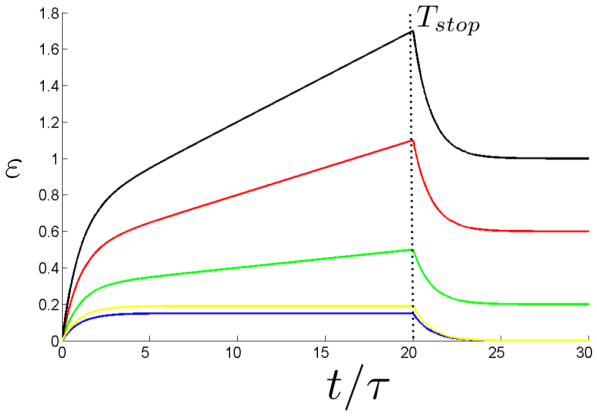

FIG. 4: Creep curves. A constant stress σ is applied from time $t = 0$ to $T_{stop} = 20\tau$ (vertical dashed line), where $\tau = \eta_{\rm cyto}/K_{\rm cortex}$ is the viscoelastic time. The deformation ε is plotted during a transient increase, then a decrease. From bottom to top, $\sigma/\sigma_Y = 0.6$ (blue), 0.95 (yellow), 1.5 (green), 2.5 (red), 3.5 (black), where σ_Y is the yield stress.

rearrange; the tissue flows like a liquid with a viscosity η_Y much larger than $\eta_{\rm cyto}$.

The existence of a yield stress σ_Y results from the fact that cells, considered as visco-elastic solids, need to undergo a finite deformation before triggering a rearrangement. This is similar to the behaviour of amorphous materials like foams, an important difference being that tissues generate active forces. If the tissue presents a high level of active forces, generated by cell divisions and apoptoses [6] and more generally by molecular motors, the cells undergo several rearrangements which can in practice have the effect of lowering the yield stress σ_Y [7].

According to Fig. 3, we have $\varepsilon = \varepsilon_{\rm intra} + \varepsilon_{\rm inter}$. Here, $\dot\varepsilon_{\rm inter}$ and $\dot\varepsilon_{\rm intra}$ respectively correspond to the 1D projections of the plastic deformation rate $\overline{\overline{\mathbf{D}}}_p$ and of the deformation rate $\dot{\overline{\mathbf{e}}}$.

The energy and dissipation functions of the independent variables ε and $\varepsilon_{\rm inter}$ can be written as:

$$\mathcal{E}(\varepsilon,\varepsilon_{\rm inter}) = \frac{1}{2}K_{\rm cortex}(\varepsilon-\varepsilon_{\rm inter})^2 \quad (23)$$

$$\mathcal{D}(\dot\varepsilon,\dot\varepsilon_{\rm inter}) = \frac{1}{2}\eta_{\rm cyto}(\dot\varepsilon-\dot\varepsilon_{\rm inter})^2+\frac{1}{2}\eta_Y(\dot\varepsilon_{\rm inter})^2 +\sigma_Y|\dot\varepsilon_{\rm inter}| \quad (24)$$

where $\dot\varepsilon_{\rm inter} = 0$ when $|\sigma| < \sigma_Y$. From Eqs. (9,10) we obtain

$$\sigma = \frac{\partial\mathcal{D}}{\partial\dot\varepsilon}+\frac{\partial\mathcal{E}}{\partial\varepsilon} = K_{\rm cortex}(\varepsilon-\varepsilon_{\rm inter})+\eta_{\rm cyto}(\dot\varepsilon-\dot\varepsilon_{\rm inter}) \quad (25)$$

$$0 = \frac{\partial\mathcal{D}}{\partial\dot\varepsilon_{\rm inter}}+\frac{\partial\mathcal{E}}{\partial\varepsilon_{\rm inter}} = \eta_{\rm cyto}(\dot\varepsilon_{\rm inter}-\dot\varepsilon)+\eta_Y(\dot\varepsilon_{\rm inter}) +K_{\rm cortex}(\varepsilon_{\rm inter}-\varepsilon)+\sigma_Y\frac{\dot\varepsilon_{\rm inter}}{|\dot\varepsilon_{\rm inter}|} \quad (26)$$

In a creep experiment, a stress σ is maintained constant until a time T_{stop}. The relaxation then starts and the deformation decreases. Fig. 4 represents creep curves, *i.e.* the total deformation ε solution of Eqs. (25-26) in a creep experiment. The individual cells are deformed as viscoelastic solids. If the magnitude of the applied stress σ is lower than the yield stress σ_Y, the deformation ε reaches a plateau, and when σ is brought back to zero the deformation ε relaxes back to zero over a time $\tau = \eta_{\rm cyto}/K_{\rm cortex}$: this viscoelastic time τ is the natural timescale of the material. If σ is larger than the yield stress σ_Y, plasticity occurs, the adhesions between cells break and the cells rearrange. After a typical time τ, cell shapes reach their maximal deformation, so that afterwards the tissue flows only due to cell rearrangements: the deformation ε steadily increases. When σ is brought back to zero the cell shapes relax to equilibrium within a time τ but the total deformation ε does not relax back to zero.

B. Growth

A tissue can grow by a combination of two processes : each cell rest size may increae; or the cell number may increase by cell division. We illustrate the latter case with a 1D example where we assume that after a full cell cycle the rest lengths ℓ_0 of the daughter cells are eventually identical to that of the mother cell. Cell divisions can affect the tissue mechanics if the duration of an experiment is of the order of, or larger than, the inverse of the division rate (typically one day for epithelial cells [82]).

At cell scale, and independently of its biological origin and regulation, a cell division is mathematically speaking a topological process, by which the rest state of a cell is discontinuously replaced by the rest state of two

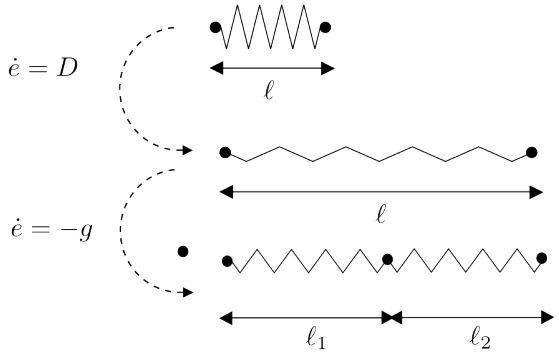

FIG. 5: Schematic one dimensional representation of a dividing cell. A cell changes its size ℓ by stretching (from top to center). It then divides, yielding two daughter cells of the same total size $\ell_1 + \ell_2$ (from center to bottom). Each cell has the same rest length ℓ_0, so that the division changes the rest length from ℓ_0 to $2\ell_0$. Notations $\dot{e}$, D, g refer to the continuum description: upon coarse-graining at the tissue scale, the discontinuities at the cell scale are wiped out. Stretching is characterised by the deformation rate D which increases the elastic deformation ($\dot{e} = D > 0$) and division by the growth rate g which relieves it ($\dot{e} = -g < 0$).

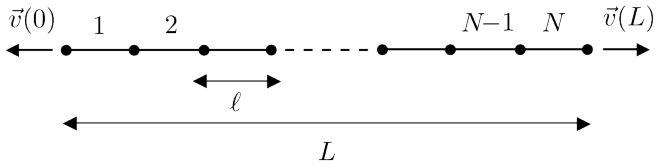

FIG. 6: Notations for the discrete approach of growth (Section III B 1). A one dimensional tissue of length L is made of N cells of length ℓ.

cells (Fig. 5). The net result is an irreversible change in the rest state of the tissue, with an increase in the sum of the cell rest sizes, and thus a decrease in the tissue deformation. The associated mechanical description is decomposed into two steps: the cell elastic deformation e is not only increased by stretching but also decreased by tissue growth, see Fig. 5. Note that after the division, the daughter cells can in turn change size and/or divide again.

We now study a tissue where cells, described as elastic, divide and/or die. For simplicity, we first study a linear regime in 1D at the cell scale using a discrete approach (Section III B 1), then a continuum description (Section III B 2), and finally incorporate the tensorial nature of growth with the corresponding objective derivatives into PDEs (Section III B 3).

1. *Discrete approach*

Let us consider a 1D tissue of length L, made of N cells of length ℓ (Fig. 6) and rest length ℓ_0:

$$L = N\ell \tag{27}$$

The evolutions of these three quantities are related through:

$$\frac{\mathrm{d}L}{\mathrm{d}t} = \ell\frac{\mathrm{d}N}{\mathrm{d}t} + N\frac{\mathrm{d}\ell}{\mathrm{d}t} \tag{28}$$

which we rewrite as:

$$\frac{\mathrm{d}\ell}{\mathrm{d}t} = \frac{\mathrm{d}L/\mathrm{d}t}{N} - \frac{\mathrm{d}N/\mathrm{d}t}{N}\,\frac{L}{N} \tag{29}$$

We now determine the l.h.s. of Eq. (29) by estimating both terms of its r.h.s. The evolution equation of N is:

$$\frac{\mathrm{d}N}{\mathrm{d}t} = g\,N \tag{30}$$

where the growth rate g is the balance between division rate k_d and apoptosis rate k_a (see Appendix E for their operational definitions):

$$g = k_d - k_a \tag{31}$$

Meanwhile, the time derivative of L is the difference in velocities between both ends:

$$\frac{\mathrm{d}L}{\mathrm{d}t} = v(L) - v(0) = DL \tag{32}$$

where D is the Eulerian elongation rate (Eq. 16):

$$D \equiv \frac{v(L) - v(0)}{L} \tag{33}$$

Combining Eqs. (29), (30) and (32) yields the time evolution of ℓ:

$$\frac{\mathrm{d}\ell}{\mathrm{d}t} = (D - g)\,\ell \tag{34}$$

The cell elongation rate is the difference between the tissue elongation rate and the growth rate.

2. *Continuum mechanics approach*

We now link the discrete formulation (Section III B 1) to a continuum one. We use the cell elongation $\ell - \ell_0$ to define the elastically stored part of the deformation

(defined in Section II C). Within a linear approximation valid for small deformations:

$$e \equiv \frac{\ell - \ell_0}{\ell_0} \tag{35}$$

Assuming that ℓ_0 is constant, and combining Eqs. (34) with (35), we get:

$$\begin{aligned} \dot{e} &= (D-g)\frac{\ell}{\ell_0} \\ &= (1+e)(D-g) \\ &\simeq D-g \end{aligned} \tag{36}$$

still in the limit of small elastic deformations. Eq. (35) admits several possible generalisations at large deformations, each of which in turn yields a slightly different version of Eq. (36).

The elastic modulus of a domain of tissue is:

$$G \equiv K\,\ell_0 \tag{37}$$

where K is the spring constant of one cell and ℓ_0 is its rest length:

$$\sigma = K\ (\ell - \ell_0) \tag{38}$$

Combining Eqs. (35) and (37) yields the continuum elasticity equation:

$$\sigma = G\,e \tag{39}$$

Combining Eqs. (36,38,39) yields the stress evolution equation:

$$\dot{\sigma} \simeq G\,(D-g) \tag{40}$$

Eq. (40) shows that as expected, the stress, when tensile, increases when the tissue is subjected to elongation (Eq. 33) and decreases when the growth rate g (Eq. 30) increases the tissue rest length; see [83, 84] for a similar approach.

Eq. (40) can be associated to a rheological diagram as follows. Consider a motor working at constant deformation rate g in series with a spring of constant $k = G$ (Fig. 7). D and e denote respectively the total deformation rate and the deformation of the spring: $\dot{e} = D - g$. Combined with Eq. (39), this yields Eq. (40). This can also be treated within the dissipation function formalism, see Section III C.

Growth should be taken into account in the mass conservation equation through the source term $s = g\,\rho$, so that Eq. (17) becomes:

$$\left(\frac{\partial}{\partial t} + v\frac{\partial}{\partial x}\right)\rho + \rho\frac{\partial v}{\partial x} = g\,\rho \tag{41}$$

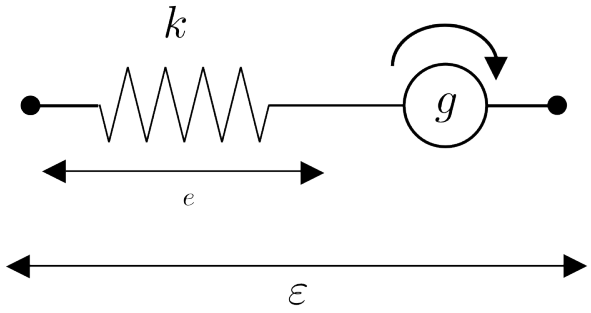

FIG. 7: Model for growth in the presence of elasticity. The deformation rate g is constant, and the spring has a stiffness k.

3. Growth in higher dimension

We now extend the 1D, scalar description of growth (Section III B 2) to incorporate more spatial dimensions. Eq. (36) is generalized using Eq. (19): see Appendix D for the definition and discussion of the elastic deformation tensor $\overline{\overline{\mathbf{e}}}$. The evolution of the elastic deformation now reads:

$$\dot{\overline{\overline{\mathbf{e}}}} = \overline{\overline{\mathbf{D}}} + \nabla\vec{v}\,\overline{\overline{\mathbf{e}}} + \overline{\overline{\mathbf{e}}}\,\nabla\vec{v}^T - \overline{\overline{\mathbf{g}}} \tag{42}$$

where the fields $\vec{v}$, $\overline{\overline{\mathbf{e}}}$, $\overline{\overline{\mathbf{D}}}$ and $\overline{\overline{\mathbf{g}}}$ depend on $(\vec{x}, t)$. The growth tensor $\overline{\overline{\mathbf{g}}}$ is mainly isotropic and changes the volume. It may however contain a component that reflects statistically oriented cell divisions. Let $\overline{\overline{\mathbf{g}}} = \overline{\overline{\mathbf{g}}}_{\rm iso} + \overline{\overline{\mathbf{g}}}_{\rm oriented}$ be the corresponding decomposition. Appendix D 4 shows that they satisfy:

$$\overline{\overline{\mathbf{g}}}_{\rm iso} \propto \left(\overline{\overline{\mathbf{I}}} + 2\overline{\overline{\mathbf{e}}}\right) \tag{43}$$

$$\mathrm{Tr}\left[\left(\overline{\overline{\mathbf{I}}} + 2\overline{\overline{\mathbf{e}}}\right)^{-1}\overline{\overline{\mathbf{g}}}_{\rm oriented}\right] = 0 \tag{44}$$

Using Eq. (42) and the relationship between stress and deformation yields the stress evolution equation. One can then incorporate it into the partial differential equations of the usual continuum mechanics framework, as in Section II D.

C. Contractility

In tissues, cell-scale contractility is often determined by the distribution of molecular motors such as myosin II. Upon coarse-graining, it translates into tissue-scale contractility. In the simplest case of a 1D description, such contractility may be modelled by adding a constant stress in parallel with the dashpot of a Maxwell rheological diagram (Fig. 8a).

Choosing ε and for instance ε_2 as independent vari-

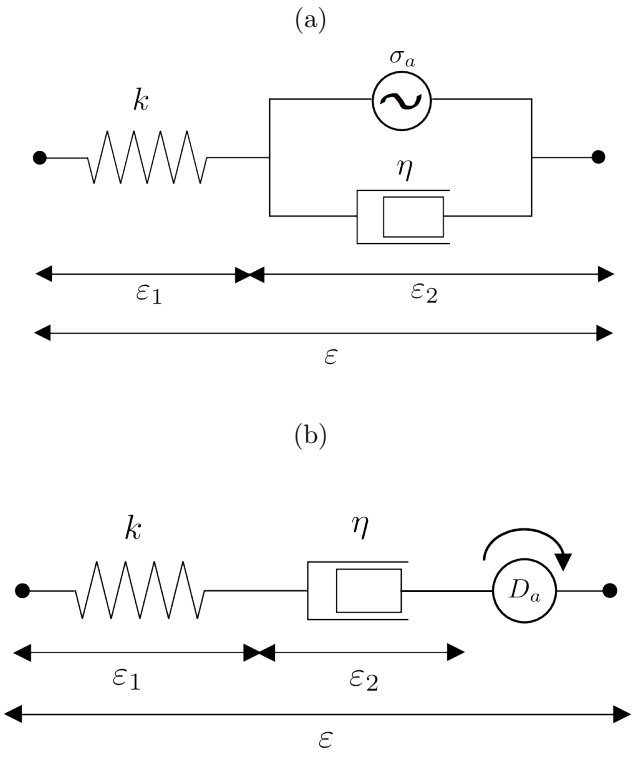

FIG. 8: Two equivalent models of contractility. (a) With a constant active stress σ_a. (b) With a constant active deformation rate D_a.

ables (with $\varepsilon = \varepsilon_1 + \varepsilon_2$), the energy and dissipation functions can be written in the form of Eqs. (7,8), with $m = 1$:

$$\mathcal{E}(\varepsilon, \varepsilon_2) = \frac{1}{2} k \varepsilon_1^2 = \frac{1}{2} k (\varepsilon - \varepsilon_2)^2 \tag{45}$$

$$\tag{46}$$

$$\mathcal{D}(\dot{\varepsilon}, \dot{\varepsilon}_2) = \frac{1}{2} \eta \dot{\varepsilon}_2^2 + \sigma_a \dot{\varepsilon}_2 \tag{47}$$

where σ_a denotes the active stress: it is positive in the case of a contracting tissue.

Eqs. (45,46) with Eqs. (9,10) yield:

$$\sigma = \frac{\partial \mathcal{D}}{\partial \dot{\varepsilon}} + \frac{\partial \mathcal{E}}{\partial \varepsilon} = k(\varepsilon - \varepsilon_2). \tag{48}$$

$$0 = \frac{\partial \mathcal{D}}{\partial \dot{\varepsilon}_2} + \frac{\partial \mathcal{E}}{\partial \varepsilon_2} = \eta \dot{\varepsilon}_2 - k(\varepsilon - \varepsilon_2) + \sigma_a \tag{49}$$

Differentiating Eq. (48) yields $\dot{\sigma} = k(\dot{\varepsilon} - \dot{\varepsilon}_2)$. Combining it with Eq. (49) yields the stress evolution equation:

$$\dot{\sigma} + \frac{1}{\tau} (\sigma - \sigma_a) = kD \tag{50}$$

where $D = \dot{\varepsilon}$, see Eq. (16), and $\tau = \eta/k$. Eq. (50) is the evolution equation of a classical Maxwell element plus a constant shift in stress due to the active stress. This is reminiscent of the active force included in Ref. [28] and corresponds to a simplified model of muscle mechanics [85]. The active stress can of course be tensorial, for instance when the spatial distribution of motors is anisotropic. This can readily be taken into account by the formalism, in analogy with continuum descriptions at the scale of the cytoskeleton [61], but now at tissue scale.

In the rheological diagram of Fig. 8b, D_a represents a constant deformation rate (negative for contractility), Such a rheological diagram has been introduced at the sub-cellular length scale, in the context of the actin/myosin cortex, and the active strain rate $\overline{\overline{\mathbf{D}}}_a$ is then interpreted in terms of the myosin concentration $c_{\rm my}$, the step length $l_{\rm my}$ of the molecular motors and the binding rate $\tau_{\rm my}$: $D_a = -c_{\rm my} l_{\rm my}/\tau_{\rm my}$ [86, 87].

Strikingly, the rheological diagram of Fig. 8b leads to the same stress evolution equation as the diagram of Fig. 8a. This can be checked easily by decomposing the total deformation rate as $\dot{\varepsilon} = \dot{\varepsilon}_1 + \dot{\varepsilon}_2 + D_a$ and by defining the energy and dissipation functions again in the form of Eqs. (7,8) with $m = 1$:

$$\mathcal{E}(\varepsilon, \varepsilon_1) = \frac{1}{2} k \varepsilon_1^2 \tag{51}$$

$$\mathcal{D}(\dot{\varepsilon}, \dot{\varepsilon}_1) = \frac{1}{2} \eta \dot{\varepsilon}_2^2 = \frac{1}{2} \eta (\varepsilon - \dot{\varepsilon}_1 - D_a)^2 \tag{52}$$

Injecting Eqs. (51,52) into Eqs. (9,10) and differentiating σ with respect to time yields:

$$\dot{\sigma} + \frac{\sigma}{\tau} = k (D - D_a) \tag{53}$$

where $D = \dot{\varepsilon}$, see Eq. (16). This equation is the same as Eq. (50) if σ_a/τ is replaced by $-kD_a$. The two rheological diagrams given by Fig. 8 are thus equivalent (see another example in Appendix B).

D. Coupling non-mechanical fields to a rheological model

Suppose we need to include an additional, non-mechanical field, distinct from the rheological scheme. The dissipation function formalism allows to postulate forms of the energy and dissipation functions that respect the symmetries of the system, and take into account the scalar, polar, axial or tensorial nature of the non-mechanical field (see definitions in Appendix C). It provides a framework within which various couplings between fields may be introduced in a systematic manner.

In the following, we present worked-out, simple examples that involve such couplings, in relation to a viscous or viscoelastic rheology, and may be relevant to the description of specific tissues. Of course, more complex couplings may be considered whenever needed, that also involve other ingredients such as plasticity, tissue growth

or cell contractility.

1. Scalar field

The simplest instance of a scalar field is arguably the concentration field c of a morphogen [11] or of a relevant signaling molecule (see Ref. [88] for a more complex case). The energy $\mathcal{E}$ and the dissipation function $\mathcal{D}$ depend on the fields $(\varepsilon, \varepsilon_k, c)$ and $(\varepsilon, \dot{\varepsilon}_k, \dot{c})$, respectively.

Let us treat a simple example which couples the scalar field to the mechanical fields through the dissipation function. In one spatial dimension, we consider the case of a Maxwell viscoelastic liquid (Fig. 9), with total deformation $\varepsilon = \varepsilon_1 + \varepsilon_2$, where ε_1, ε_2 denote the deformation of the spring and of the dashpot, respectively. Its usual evolution equation $\dot{\sigma} + \sigma/\tau = kD$ (when subjected to deformation rate $D = \dot{\varepsilon}$) is modified in the presence of a coupled field, for instance a morphogen concentration c.

We choose for instance ε and ε_2 as independent variables together with c and write functions of the same form as Eqs. (7,8) with $m = 2$ additional internal variables:

$$\mathcal{E}(\varepsilon, \varepsilon_2, c) = \frac{1}{2}k(\varepsilon - \varepsilon_2)^2 + \frac{1}{2}\chi c^2 \tag{54}$$

$$\mathcal{D}(\dot{\varepsilon}, \dot{\varepsilon}_2, \dot{c}) = \frac{1}{2}\eta\dot{\varepsilon}_2^2 + \frac{1}{2}\xi\dot{c}^2 + \omega\dot{\varepsilon}_2\dot{c} \tag{55}$$

In Eqs. (54,55) we choose to couple the concentration c to the deformation ε_2 through their time derivatives, with a dissipative coupling coefficient ω. This and other similar choices made below would need to be carefully validated by comparison with experimental data in specific cases. To ensure the convexity of the dissipation function, the parameters k, χ, η and ξ are non-negative, and the following inequality holds:

$$\omega^2 \leq \xi\eta \tag{56}$$

Eqs. (9,10) yield here the expression of the stress:

$$\sigma = \frac{\partial \mathcal{D}}{\partial \dot{\varepsilon}} + \frac{\partial \mathcal{E}}{\partial \varepsilon} = k(\varepsilon - \varepsilon_2) \tag{57}$$

and two variational equations:

$$0 = \frac{\partial \mathcal{D}}{\partial \dot{\varepsilon}_2} + \frac{\partial \mathcal{E}}{\partial \varepsilon_2} = \eta\dot{\varepsilon}_2 - k(\varepsilon - \varepsilon_2) + \omega\dot{c} \tag{58}$$

$$0 = \frac{\partial \mathcal{D}}{\partial \dot{c}} + \frac{\partial \mathcal{E}}{\partial c} = \xi\dot{c} + \chi c + \omega\dot{\varepsilon}_2. \tag{59}$$

Injecting Eq. (57) and its time derivative into Eq. (58), we find the evolution equation for the stress field:

$$\dot{\sigma} + \frac{\sigma}{\tau} = kD + \frac{k\omega}{\eta}\dot{c} \tag{60}$$

where the viscoelastic time is $\tau = \eta/k$ and where $D = \dot{\varepsilon}$, see Eq. (16). Similarly, eliminating $\dot{\varepsilon}_2$ between Eqs. (58) and (59), then injecting Eq. (57), we find the evolution equation for the scalar field c:

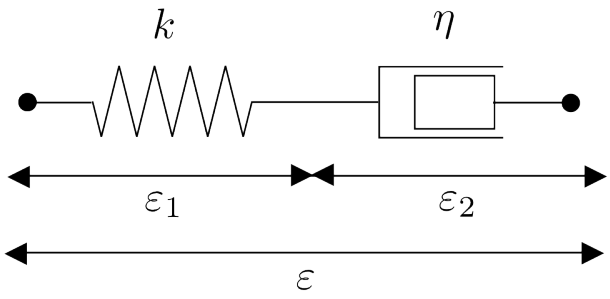

FIG. 9: A Maxwell viscoelastic liquid.

$$\dot{c} + \frac{c}{\tau_c} = -\frac{\omega}{\eta\xi - \omega^2}\,\sigma \tag{61}$$

with a relaxation time

$$\tau_c = \frac{\xi\eta - \omega^2}{\chi\eta} \tag{62}$$

Here τ_c is positive due to Eq. (56) and its inverse τ_c^{-1} can be the degradation rate of the morphogen. Using (61), we eliminate $\dot{c}$ in (60) and find:

$$\dot{\sigma} + \frac{\sigma}{\tau_\sigma} = kD - \frac{k\omega\chi}{\eta\xi - \omega^2}c \tag{63}$$

where the stress relaxation time

$$\tau_\sigma = \frac{\xi\eta - \omega^2}{\xi k} \tag{64}$$

is shorter than the usual viscoelastic time $\tau = \eta/k$ as soon as the coupling ω is non-zero. Eqs. (61,63) provide an Eulerian formulation of the system evolution in terms of the deformation rate D.

In the long time limit, the rheology is viscous:

$$\sigma \to \eta\, D \tag{65}$$

$$c \to \frac{\omega}{\chi}\, D \tag{66}$$

and all relevant fields are proportional to each other in this linear regime.

2. Polar field

Relevant non-mechanical fields may not always be scalar: they can for instance be polar or axial (Appendix C). For instance, in collectively migrating cells, a cell acquires a front-rear asymmetry manifested both in its shape and in intracellular protein distributions. Such cell-scale asymmetry defines a vector field, the polarity $\vec{p}$

[48, 49], where $\vec{p}$ and $-\vec{p}$ characterize opposite configurations. This is an example of a polar orientational order parameter.

We treat here for simplicity a case with one dimension of space, where the polarity $\vec{p} = p(x,t)\,\vec{e}_x$ ($\vec{e}_x$ is a unit vector) couples to a Maxwell viscoelastic liquid (see Fig. 9 for the notations). The energy $\mathcal{E}$ and the dissipation function $\mathcal{D}$ depend on the fields $(\varepsilon, \varepsilon_1, p)$ and $(\dot\varepsilon, \dot\varepsilon_1, \dot p)$, respectively. When homogeneous polarity is preferred, the energy functional includes a term accounting for the cost of inhomogeneities of the polarity, with a prefactor (called "Frank constant") $K_{\rm F} \geq 0$ [60]. The system is invariant under the transformation $x \to -x$, $p \to -p$, allowing for a coupling term between deformation and polarity gradient in the energy function. Eqs. (7,8) read, with $m = 2$:

$$\begin{aligned}\mathcal{E}(\varepsilon, \varepsilon_1, p) &= \frac{1}{2} k \varepsilon_1^2 + \frac{1}{2}\chi p^2 \\ &\quad + \frac{1}{2} K_{\rm F} \left(\frac{\partial p}{\partial x}\right)^2 + \omega\, \varepsilon_1 \frac{\partial p}{\partial x} \end{aligned} \tag{67}$$

where k, χ, $K_{\rm F}$ are non-negative parameters, and where ω is a parameter satisfying the condition $\omega^2 \leq k K_{\rm F}$ imposed by the convexity of $\mathcal{E}$. The simplest expression for the dissipation function has no cross-coupling:

$$\mathcal{D}(\dot\varepsilon, \dot\varepsilon_1, \dot p) = \frac{1}{2}\eta(\dot\varepsilon - \dot\varepsilon_1)^2 + \frac{1}{2}\xi \dot p^2 \tag{68}$$

where η and ξ are non-negative parameters. The stress now depends on the polarity gradient:

$$\sigma = \frac{\partial \mathcal{D}}{\partial \dot\varepsilon} + \frac{\partial \mathcal{E}}{\partial \varepsilon} = \eta(\dot\varepsilon - \dot\varepsilon_1) \tag{69}$$

through the additional relationship:

$$0 = \frac{\partial \mathcal{D}}{\partial \dot\varepsilon_1} + \frac{\partial \mathcal{E}}{\partial \varepsilon_1} = -\eta(\dot\varepsilon - \dot\varepsilon_1) + k\varepsilon_1 + \omega \frac{\partial p}{\partial x} \tag{70}$$

The variational equation for the polar field is obtained after integration by parts:

$$0 = \frac{\partial \mathcal{D}}{\partial \dot p} + \frac{\partial \mathcal{E}}{\partial p} = \xi \dot p + \chi p - K_{\rm F}\frac{\partial^2 p}{\partial x^2} - \omega \frac{\partial \varepsilon_1}{\partial x} \tag{71}$$

Combining Eqs. (69-71) we obtain a set of two coupled evolution equations for the stress and polarity field:

$$\begin{aligned}\dot\sigma + \frac{k}{\eta}\sigma &= kD + \frac{\omega^2}{k\xi}\frac{\partial^2 \sigma}{\partial x^2} - \frac{\omega\chi}{\xi}\frac{\partial p}{\partial x} \\ &\quad + \omega \frac{k K_{\rm F} - \omega^2}{k\xi}\frac{\partial^3 p}{\partial x^3} \end{aligned} \tag{72}$$

$$\dot p + \frac{\chi}{\xi} p = \frac{\omega}{k\xi}\frac{\partial \sigma}{\partial x} + \frac{k K_{\rm F} - \omega^2}{k\xi}\frac{\partial^2 p}{\partial x^2} \tag{73}$$

with $D = \dot\varepsilon$, see Eq. (16). The relaxation times for the polarity and stress are distinct. Eqs. (72,73) combined with mechanical balance $\partial\sigma/\partial x = 0$ may be solved numerically once accompanied by relevant boundary conditions. See Ref. [89] for a similar treatment also including active couplings between the polar and mechanical fields.

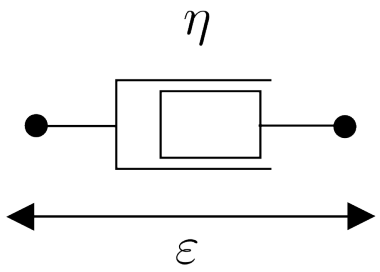

FIG. 10: Viscous fluid.

3. *Tensor field*

Variables such as stress which require force measurements are called dynamical quantities. On the opposite, some variables can be determined from visual measurement only: they are called static or kinematic if they can be determined from still images or movies, respectively. They are descriptive: their measurement do not require any proper knowledge of either the physics or the biology that underly the system behaviour, nor of the past history of the system. In epithelia, an example is given by noting that planar cell polarity proteins exhibit tissue-scale ordered domains that are often best described by a tensor field [15, 16]. These tensors, and other similar ones (see Appendix A), should be added to a consistent continuum modelling of a cellular material, for instance as variables of the energy and dissipation functions. See also Refs. [90, 91] for a detailed study, within a variational framework, of the derivation of constitutive equations involving a tensorial order parameter.

Here, we treat the case of a viscous liquid (Fig. 10), and choose to couple the deformation rate tensor $\overline{\overline{\mathbf{D}}}$ to a second-order tensor $\overline{\overline{\mathbf{Q}}}$ in the dissipation function. Formally, Eqs. (7,8) should be written with an additional internal variable $\overline{\overline{\mathbf{Q}}}$, so that $m = 1$, and tensorial coupling parameters. However, the trace and the deviators of tensors (here $\overline{\overline{\mathbf{D}}}$ and $\overline{\overline{\mathbf{Q}}}$) are largely independent; in practice it is convenient to treat the trace and the deviator as separate variables with distinct, scalar coupling

parameters. Eqs. (7,8) thus read, with $m = 2$:

$$\mathcal{E}(\mathrm{Dev}\overline{\overline{\mathbf{Q}}}, \mathrm{Tr}\overline{\overline{\mathbf{Q}}}) = \frac{1}{2}\chi\left(\mathrm{Dev}\overline{\overline{\mathbf{Q}}}\right)^2 + \frac{1}{2}\bar{\chi}\left(\mathrm{Tr}\overline{\overline{\mathbf{Q}}}\right)^2 \quad (74)$$

$$\mathcal{D}(\mathrm{Dev}\overline{\overline{\mathbf{D}}}, \mathrm{Tr}\overline{\mathbf{D}}, \mathrm{Dev}\dot{\overline{\overline{\mathbf{Q}}}}, \mathrm{Tr}\dot{\overline{\mathbf{Q}}}) = \frac{1}{2}\eta\left(\mathrm{Dev}\overline{\overline{\mathbf{D}}}\right)^2 + \frac{1}{2}\bar{\eta}\left(\mathrm{Tr}\overline{\overline{\mathbf{D}}}\right)^2 + \frac{1}{2}\xi\left(\mathrm{Dev}\dot{\overline{\overline{\mathbf{Q}}}}\right)^2 + \frac{1}{2}\bar{\xi}\left(\mathrm{Tr}\dot{\overline{\mathbf{Q}}}\right)^2 + \omega\,\mathrm{Dev}\overline{\overline{\mathbf{D}}}\,\mathrm{Dev}\dot{\overline{\overline{\mathbf{Q}}}} + \bar{\omega}\,\mathrm{Tr}\overline{\mathbf{D}}\,\mathrm{Tr}\dot{\overline{\mathbf{Q}}} \quad (75)$$

The parameters χ, $\bar{\chi}$, η, $\bar{\eta}$, ξ, $\bar{\xi}$ are non-negative, and the inequalities $\omega^2 \leq \xi\eta$, $\bar{\omega}^2 \leq \bar{\xi}\bar{\eta}$ ensure the convexity of the dissipation function. From Eqs. (9,10) we first compute the stress tensor:

$$\mathrm{Dev}\overline{\overline{\sigma}} = \frac{\partial\mathcal{D}}{\partial\mathrm{Dev}\overline{\overline{\mathbf{D}}}} = \eta\mathrm{Dev}\overline{\overline{\mathbf{D}}} + \omega\mathrm{Dev}\dot{\overline{\overline{\mathbf{Q}}}} \quad (76)$$

$$\mathrm{Tr}\overline{\overline{\sigma}} = \frac{\partial\mathcal{D}}{\partial\mathrm{Tr}\overline{\mathbf{D}}} = \bar{\eta}\mathrm{Tr}\overline{\overline{\mathbf{D}}} + \bar{\omega}\mathrm{Tr}\dot{\overline{\overline{\mathbf{Q}}}} \quad (77)$$

where a linear coupling to $\dot{\overline{\overline{\mathbf{Q}}}}$ modifies the usual constitutive equations of a viscous liquid. We next obtain the variational equations:

$$0 = \frac{\partial\mathcal{D}}{\partial\mathrm{Dev}\dot{\overline{\overline{\mathbf{Q}}}}} + \frac{\partial\mathcal{E}}{\partial\mathrm{Dev}\overline{\overline{\mathbf{Q}}}} = \xi\mathrm{Dev}\dot{\overline{\overline{\mathbf{Q}}}} + \omega\mathrm{Dev}\overline{\overline{\mathbf{D}}} + \chi\mathrm{Dev}\overline{\overline{\mathbf{Q}}} \quad (78)$$

$$0 = \frac{\partial\mathcal{D}}{\partial\mathrm{Tr}\dot{\overline{\mathbf{Q}}}} + \frac{\partial\mathcal{E}}{\partial\mathrm{Tr}\overline{\overline{\mathbf{Q}}}} = \bar{\xi}\mathrm{Tr}\dot{\overline{\overline{\mathbf{Q}}}} + \bar{\omega}\mathrm{Tr}\overline{\overline{\mathbf{D}}} + \bar{\chi}\mathrm{Tr}\overline{\overline{\mathbf{Q}}} \quad (79)$$

from which the evolution equations for the tensor $\overline{\overline{\mathbf{Q}}}$ read:

$$\mathrm{Dev}\dot{\overline{\overline{\mathbf{Q}}}} + \frac{\chi}{\xi}\mathrm{Dev}\overline{\overline{\mathbf{Q}}} = -\frac{\omega}{\xi}\mathrm{Dev}\overline{\overline{\mathbf{D}}} \quad (80)$$

$$\mathrm{Tr}\dot{\overline{\mathbf{Q}}} + \frac{\bar{\chi}}{\bar{\xi}}\mathrm{Tr}\overline{\overline{\mathbf{Q}}} = -\frac{\bar{\omega}}{\bar{\xi}}\mathrm{Tr}\overline{\overline{\mathbf{D}}} \quad (81)$$

Note that the relaxation times for the trace and deviator can in principle be different. Inserting (80-81) into (76-77) yields the stress tensor:

$$\mathrm{Dev}\overline{\overline{\sigma}} = \left(\eta - \frac{\omega^2}{\xi}\right)\mathrm{Dev}\overline{\overline{\mathbf{D}}} - \frac{\omega\chi}{\xi}\mathrm{Dev}\overline{\overline{\mathbf{Q}}} \quad (82)$$

$$\mathrm{Tr}\overline{\overline{\sigma}} = \left(\bar{\eta} - \frac{\bar{\omega}^2}{\bar{\xi}}\right)\mathrm{Tr}\overline{\overline{\mathbf{D}}} - \frac{\bar{\omega}\bar{\chi}}{\bar{\xi}}\mathrm{Tr}\overline{\overline{\mathbf{Q}}} \quad (83)$$

In the long time limit, we find for the tensor $\overline{\overline{\mathbf{Q}}}$:

$$\mathrm{Dev}\overline{\overline{\mathbf{Q}}} \to -\frac{\omega}{\chi}\mathrm{Dev}\overline{\overline{\mathbf{D}}} \quad (84)$$

$$\mathrm{Tr}\overline{\overline{\mathbf{Q}}} \to -\frac{\bar{\omega}}{\bar{\chi}}\mathrm{Tr}\overline{\overline{\mathbf{D}}} \quad (85)$$

(compare with Eq. (66)), and for the viscous stress tensor:

$$\mathrm{Dev}\overline{\overline{\sigma}} \to \eta\mathrm{Dev}\overline{\overline{\mathbf{D}}} \quad (86)$$

$$\mathrm{Tr}\overline{\overline{\sigma}} \to \bar{\eta}\mathrm{Tr}\overline{\overline{\mathbf{D}}} \quad (87)$$

(compare with Eq. (65)). Ref. [16] provides a study of Eq. (84), where the tensor $\overline{\overline{\mathbf{Q}}}$ quantifies the polarization of the Dachs protein in the dorsal thorax of fruitfly pupae.

IV. CONCLUSION

Starting from physical insights and symmetry considerations, we are able to write down tensorial constitutive equations and to insert them in the framework of continuum mechanics. Here is one example of the possible form of these equations:

$$\frac{\partial\rho}{\partial t} + \nabla\cdot(\rho\vec{v}) = s \quad (88)$$

$$\nabla\cdot\overline{\overline{\sigma}}(\vec{x},t) + \vec{f}(\vec{x},t) = \vec{0} \quad (89)$$

$$\overline{\overline{\sigma}} = F\left(\overline{\overline{\mathbf{e}}}, \overline{\overline{\mathbf{D}}}, \nabla, \ldots\right) \quad (90)$$

$$\dot{\overline{\overline{\mathbf{e}}}} = \overline{\overline{\mathbf{D}}} + \nabla\vec{v}\,\overline{\overline{\mathbf{e}}} + \overline{\overline{\mathbf{e}}}\,\nabla\vec{v}^T - \overline{\overline{\mathbf{g}}} - \overline{\overline{\mathbf{D}}}_p - \overline{\overline{\mathbf{D}}}_a \quad (91)$$

where $\overline{\overline{\mathbf{g}}}$ is the growth rate, $\overline{\overline{\mathbf{D}}}_p$ the plastic deformation rate, and $\overline{\overline{\mathbf{D}}}_a$ the active deformation rate. When the constitutive relations are linear, this whole approach boils down to the classical framework of hydrodynamics. In the presence of plasticity, non-differentiable rheological elements (sliders) are treated using the dissipation function formalism. Ingredients specific to living tissues, such as cell contractility or division, can be straightforwardly included in a consistent manner. Further, non-mechanical features can be naturally coupled to the mechanics in a systematic way in accordance with symmetry principles. A complete set of partial differential equations modelling the system can be explicitly derived from the energy and dissipation functions, using the method described in Section II B 3, and can then be solved numerically. Section III D shows how to formally treat a large variety of biomechanical problems.

Tools exist to analyse 2D or 3D movies of tissue dynamics and perform quantitative measurements within a continuum mechanics description, so that data can be compared with the model predictions, *i.e.* numerical solutions of the model equations. Such a comparison is instrumental in determining the value of the unknown parameters, and is indeed already possible on a large scale

in animal as well as in vegetal tissues. Computing the difference(s) between wild-type tissues and other conditions, using either mutants or drugs, enables to delineate separately the contribution of a single ingredient within a complex feedback network, and to further validate a model. It is essential to limit the number of mechanical parameters, which should be much lower than the number of measurements available to constrain the models. In this respect, the continuum description is more economical than a simulation of a whole tissue at the cell scale. This advantage may be crucial when, *e.g.*, studying feedbacks between gene expression and mechanical response. *In situ* measurements of local force and stress are improving at a quick pace and will hopefully be soon compared with local elastic deformation measurements. Our modelling approach should help exploit the future wealth of available data and incorporate it into a consistent picture.

In practice, many issues need to be overcome in order to validate continuum descriptions of tissues from experimental data. First, an optimal length scale of measurement must be properly defined, larger that the typical cell size, but smaller than the sample size, and therefore suitable for hydrodynamics. Second, in heterogeneous time-dependent systems like tissues, it is also often difficult to average over space or time to improve the signal-to-noise ratio. It may then be necessary to ensemble-average several experiments performed in identical conditions, at the cost of underestimating the intrinsic behavioural variability of a living tissue. A third difficulty originates in the very size of data, in terms of manipulation and representation. Fourth, the formalism of generalised standard materials, initially developed for hard condensed matter, will probably require specific modelling efforts to incorporate features of soft condensed matter and biophysics, such as progressive plasticity [92] or cell contour fluctuations [7].

Facing this formidable task, it is important to determine the best approach in representing and correlating various fields, to obtain a more intuitive grasp of the relative importance of various couplings. Simplifications may also help, *e.g.*, replacing symmetric tensors or even vectors by scalars, assuming that amorphous materials have isotropic moduli, etc. These simplifications can only be informed by the specifics of any given system. Quite generally, genetic engineering or pharmacological treatment can help discriminate the contribution made by a particular ingredient (*e.g.*, by subtraction). Reference [16] includes some examples of scale determination, choices of simplifications, handling of data correlations when a prefactor is unknown, maps of variables and correlations, and the subtractive method.

Ultimately, numerical estimates for the parameters are needed in order to validate a model. Questions that need be considered are among the following, especially in the more distant perspective of integrating ingredients from genetics with mechanical models to fully understand morphogenetic processes. What kind of model parameters can be extracted from state-of-the art experimental data? What minimal set of data is required for extracting the parameters associated with a given class of models? Or reciprocally, given a modelling framework, what set of minimal experiments are necessary for validation and parameter extraction? Can we discriminate among models on the base of their capacity to interprete the data in the most economical way?

Acknowledgements

It is a pleasure to thank Isabelle Bonnet for a critical reading of the manuscript, and to acknowledge stimulating discussions with Hélène Delanoë and Ibrahim Cheddadi.

[1] Y.C. Fung. *Biomechanics: Mechanical Properties of Living Tissues*. Springer Verlag, 2010.

[2] Gabor Forgacs and Stuart A. Newman. *Biological Physics of the Developing Embryo*. Cambridge University Press, 2005.

[3] Carl-Philipp Heisenberg and Yohanns Bellaïche. Forces in tissue morphogenesis and patterning. *Cell*, 153:948–962, 2013.

[4] Ian W. Hamley. *Introduction to Soft Matter. Polymers, Colloids, Amphiphiles and Liquid Crustals*. John Wiley and Sons, 2010.

[5] G Forgacs, R A Foty, Y Shafrir, and M S Steinberg. Viscoelastic properties of living embryonic tissues: a quantitative study. *Biophys J*, 74:2227–2234, 1998.

[6] Jonas Ranft, Markus Basan, Jens Elgeti, Jean-François Joanny, Jacques Prost, and Frank Jülicher. Fluidization of tissues by cell division and apoptosis. *Proc Natl Acad Sci U S A*, 107:20863–20868, 2010.

[7] Philippe Marmottant, Abbas Mgharbel, Jos Käfer, Benjamin Audren, Jean-Paul Rieu, Jean-Claude Vial, Boudewijn van der Sanden, Athanasius F M Marée, François Graner, and Hélène Delanoë-Ayari. The role of fluctuations and stress on the effective viscosity of cell aggregates. *Proc Natl Acad Sci U S A*, 106:17271–17275, 2009.

[8] Fabien Montel, Morgan Delarue, Jens Elgeti, Laurent Malaquin, Markus Basan, Thomas Risler, Bernard Cabane, Danijela Vignjevic, Jacques Prost, Giovanni Cappello, and Jean-François Joanny. Stress clamp experiments on multicellular tumor spheroids. *Phys Rev Lett*, 107:188102, 2011.

[9] Loïc LeGoff, Hervé Rouault, and Thomas Lecuit. A global pattern of mechanical stress polarizes cell divisions and cell shape in the growing drosophila wing disc. *Development*, 140:4051–4059, 2013.

[10] P Fernandez, M Maier, M Lindauer, C Kuffer, Z Stor-

chova, and AR Bausch. Mitotic spindle orients perpendicular to the forces imposed by dynamic shear. *PLoS One*, 6:e28965, 2011.

[11] Lewis Wolpert, Jim Smith, Tom Jessell, Peter Lawrence, Elizabeth Robertson, and Elliot Meyerowitz. *Principles of Development*. Oxford University Press, 2006.

[12] Nicolas Olivier, Miguel A. Luengo-Oroz, Louise Duloquin, Emmanuel Faure, Thierry Savy, Israël Veilleux, Xavier Solinas, Delphine Débarre, Paul Bourgine, Andrés Santos, Nadine Peyriéras, and Emmanuel Beaurepaire. Cell lineage reconstruction of early zebrafish embryos using label-free nonlinear microscopy. *Science*, 329:967–971, 2010.

[13] Julian Moosmann, Alexey Ershov, Venera Altapova, Tilo Baumbach, Maneeshi S. Prasad, Carole LaBonne, Xianghui Xiao, Jubin Kashef, and Ralf Hofmann. X-ray phase-contrast in vivo microtomography probes new aspects of xenopus gastrulation. *Nature*, 497:374–377, 2013.

[14] Claire Bertet, Lawrence Sulak, and Thomas Lecuit. Myosin-dependent junction remodelling controls planar cell intercalation and axis elongation. *Nature*, 429:667–671, 2004.

[15] Benoît Aigouy, Reza Farhadifar, Douglas B Staple, Andreas Sagner, Jens-Christian Röper, Frank Jülicher, and Suzanne Eaton. Cell flow reorients the axis of planar polarity in the wing epithelium of drosophila. *Cell*, 142:773–786, 2010.

[16] Floris Bosveld, Isabelle Bonnet, Boris Guirao, Sham Tlili, Zhimin Wang, Ambre Petitalot, Raphaël Marchand, Pierre-Luc Bardet, Philippe Marcq, François Graner, and Yohanns Bellaïche. Mechanical control of morphogenesis by Fat/Dachsous/Four-Jointed planar cell polarity pathway. *Science*, 336:724–727, 2012.

[17] Ortrud Wartlick, Anna Kicheva, and Marcos González-Gaitán. Morphogen gradient formation. *Cold Spring Harbor Persp. Biol.*, 1:a001255, 2009.

[18] M. Shane Hutson, Yoichiro Tokutake, Ming-Shien Chang, James W. Bloor, Stephanos Venakides, Daniel P. Kiehart, and Glenn S. Edwards. Forces for morphogenesis investigated with laser microsurgery and quantitative modeling. *Science*, 300:145–149, 2003.

[19] Isabelle Bonnet, Philippe Marcq, Floris Bosveld, Luc Fetler, Yohanns Bellaïche, and François Graner. Mechanical state, material properties and continuous description of an epithelial tissue. *J R Soc Interface*, 9:2614–2623, 2012.

[20] G. Wayne Brodland, Vito Conte, P. Graham Cranston, Jim Veldhuis, Sriram Narasimhan, M. Shane Hutson, Antonio Jacinto, Florian Ulrich, Buzz Baum, and Mark Miodownik. Video force microscopy reveals the mechanics of ventral furrow invagination in drosophila. *Proc Natl Acad Sci U S A*, 107:22111–22116, 2010.

[21] Kevin K Chiou, Lars Hufnagel, and Boris I Shraiman. Mechanical stress inference for two dimensional cell arrays. *PLoS Comput Biol*, 8:e1002512, 2012.

[22] Shuji Ishihara and Kaoru Sugimura. Bayesian inference of force dynamics during morphogenesis. *J Theor Biol*, 313C:201–211, 2012.

[23] K. Sugimura and S. Ishihara. The mechanical anisotropy in a tissue promotes ordering in hexagonal cell packing. *Development*, 140:4091–4101, 2013.

[24] Xavier Trepat, Michael R. Wasserman, Thomas E. Angelini, Emil Millet, David A. Weitz, James P. Butler, and Jeffrey J. Fredberg. Physical forces during collective cell migration. *Nat. Phys.*, 5:426–430, 2009.

[25] Thomas E. Angelini, Edouard Hannezo, Xavier Trepat, Jeffrey J. Fredberg, and David A. Weitz. Cell migration driven by cooperative substrate deformation patterns. *Phys. Rev. Lett.*, 104:168104, 2010.

[26] A Saez, E Anon, M Ghibaudo, O du Roure, J-M Di Meglio, P Hersen, P Silberzan, A Buguin, and B Ladoux. Traction forces exerted by epithelial cell sheets. *J. Phys. Cond. Mat.*, 22:194119, 2010.

[27] M. Reffay, L. Petitjean, S. Coscoy, E. Grasland-Mongrain, F. Amblard, A. Buguin, and P. Silberzan. Orientation and polarity in collectively migrating cell structures: statics and dynamics. *Biophys J*, 100:2566–2575, 2011.

[28] Xavier Serra-Picamal, Vito Conte, Romaric Vincent, Ester Anon, Dhananjay T. Tambe, Elsa Bazellieres, James P. Butler, Jeffrey J. Fredberg, and Xavier Trepat. Mechanical waves during tissue expansion. *Nat. Phys.*, 8:628–634, 2012.

[29] Andrew R Harris, Loic Peter, Julien Bellis, Buzz Baum, Alexandre J Kabla, and Guillaume T Charras. Characterizing the mechanics of cultured cell monolayers. *Proc Natl Acad Sci U S A*, 109:16449–16454, 2012.

[30] Kevin Doxzen, Sri Ram Krishna Vedula, Man Chun Leong, Hiroaki Hirata, Nir S. Gov, Alexandre J. Kabla, Benoit Ladoux, and Chwee Teck Lim. Guidance of collective cell migration by substrate geometry. *Integrative Biology*, 5:1026–1035, 2013.

[31] David Gonzalez-Rodriguez, Karine Guevorkian, Stéphane Douezan, and Françoise Brochard-Wyart. Soft matter models of developing tissues and tumors. *Science*, 338:910–917, 2012.

[32] Abbas Mgharbel, Hélène Delanoë-Ayari, and Jean-Paul Rieu. Measuring accurately liquid and tissue surface tension with a compression plate tensiometer. *HFSP Journal*, 3:213–221, 2009.

[33] Tomita Vasilica Stirbat, Sham Tlili, Thibault Houver, Catherine Barentin, Jean-Paul Rieu, and Hélène Delanoë-Ayari. Multicellular aggregates: a model system for tissue rheology. *Eur Phys J E*, 36:84, 2013.

[34] Raju Tomer, Khaled Khairy, Fernando Amat, and Philipp J Keller. Quantitative high-speed imaging of entire developing embryos with simultaneous multiview light-sheet microscopy. *Nat Methods*, 9:755–763, 2012.

[35] Tatsuzo Nagai and Hisao Honda. A dynamic cell model for the formation of epithelial tissues. *Phil. Mag. B*, 81:699–719, 2001.

[36] A. F. M. Marée, V. A. Grieneisen, and P. Hogeweg. *The Cellular Potts Model and biophysical properties of cells, tissues and morphogenesis*, pages 107–136. Single Cell-Based Models in Biology and Medicine. Birkhäuser Verlag, Basel, ed. Anderson, A. R. A. and Chaplain, M. and Rejniak, K. A., 2007.

[37] Dirk Drasdo, Stefan Hoehme, and Michael Block. On the role of physics in the growth and pattern formation of multi-cellular systems: What can we learn from individual-cell based models? *J. Stat. Phys.*, 128:287–345, 2007.

[38] Bakhtier Vasiev, Ariel Balter, Mark Chaplain, James A Glazier, and Cornelis J Weijer. Modeling gastrulation in the chick embryo: formation of the primitive streak. *PLoS One*, 5:e10571, 2010.

[39] G. Wayne Brodland, Xiaoguang Chen, Paul Lee, and Mungo Marsden. From genes to neural tube defects

(ntds): Insights from multiscale computational modeling. *HFSP Journal*, 4:142–152, 2010.

[40] Alexandre J Kabla. Collective cell migration: leadership, invasion and segregation. *J R Soc Interface*, 9:3268–3278, 2012.

[41] Markus Basan, Jens Elgeti, Edouard Hannezo, Wouter-Jan Rappel, and Herbert Levine. Alignment of cellular motility forces with tissue flow as a mechanism for efficient wound healing. *Proc Natl Acad Sci U S A*, 110:2452–2459, 2013.

[42] Néstor Sepúlveda, Laurence Petitjean, Olivier Cochet, Erwan Grasland-Mongrain, Pascal Silberzan, and Vincent Hakim. Collective cell motion in an epithelial sheet can be quantitatively described by a stochastic interacting particle model. *PLoS Comput Biol*, 9:e1002944, 2013.

[43] Dominique P. Pioletti and Lalao R. Rakotomanana. Non-linear viscoelastic laws for soft biological tissues. *Eur. J. Mech. A*, 19:749–759, 2000.

[44] Paola Nardinocchi and Luciano Teresi. On the active response of soft living tissues. *J. Elast.*, 88:27–39, 2007.

[45] Markus Basan, Jean-François Joanny, Jacques Prost, and Thomas Risler. Undulation instability of epithelial tissues. *Phys Rev Lett*, 106:158101, 2011.

[46] Karine Guevorkian, Marie-Jose Colbert, Mlanie Durth, Sylvie Dufour, and Françoise Brochard-Wyart. Aspiration of biological viscoelastic drops. *Phys Rev Lett*, 104:218101, 2010.

[47] L. Preziosi, D. Ambrosi, and C. Verdier. An elasto-viscoplastic model of cell aggregates. *J Theor Biol*, 262:35–47, 2010.

[48] Pilhwa Lee and Charles W Wolgemuth. Crawling cells can close wounds without purse strings or signaling. *PLoS Comput Biol*, 7:e1002007, 2011.

[49] Michael H. Köpf and Len M. Pismen. A continuum model of epithelial spreading. *Soft Matter*, 9:3727–3734, 2012.

[50] Erika E. Kuchen, Samantha Fox, Pierre Barbier de Reuille, Richard Kennaway, Sandra Bensmihen, Jerome Avondo, Grant M. Calder, Paul Southam, Sarah Robinson, Andrew Bangham, and Enrico Coen. Generation of leaf shape through early patterns of growth and tissue polarity. *Science*, 335:1092–1096, 2012.

[51] I. Cantat, S. Cohen-Addad, F. Elias, F. Graner, R. Höhler, O. Pitois, F. Rouyer, and A. Saint-Jalmes. *Foams: structure and dynamics*. Oxford University Press, ed. S.J. Cox, 2013.

[52] 2013.

[53] S. Bénito, C. H. Bruneau, T. Colin, C. Gay, and F. Molino. An elasto-visco-plastic model for immortal foams or emulsions. *Eur. Phys. J. E*, 25:225–251, 2008.

[54] S. Benito, F. Molino, C.-H Bruneau, T. Colin, and C. Gay. Non-linear oscillatory rheological properties of a generic continuum foam model: Comparison with experiments and shear-banding predictions. *Eur. Phys. J. E*, 35:1–17, 2012.

[55] I. Cheddadi, P. Saramito, B. Dollet, C. Raufaste, and F. Graner. Understanding and predicting viscous, elastic, plastic flows. *Eur Phys J E*, 34:1–15, 2011.

[56] C. Gay and I. Cantat. Rheology of dry liquid foams or concentrated emulsions: local network deformation versus bubble or droplet shape, a two-tensor model. *Preprint*, 2011.

[57] P.M. Chaikin and T.C. Lubensky. *Principles of condensed matter physics*. Cambridge University Press, 1995.

[58] S. R. de Groot and P. Mazur. *Non-Equilibrium Thermodynamics*. Dover Publications, 1985.

[59] P. C. Martin, O. Parodi, and P. S. Pershan. Unified hydrodynamic theory for crystals, liquid crystals, and normal fluid. *Phys. Rev. A*, 6:2401 – 2420, 1972.

[60] P. G. de Gennes and J. Prost. *The Physics of Liquid Crystals, 2nd ed.* Oxford University Press, 1993.

[61] M. C. Marchetti, J. F. Joanny, S. Ramaswamy, T. B. Liverpool, J. Prost, Madan Rao, and R. Aditi Simha. Hydrodynamics of soft active matter. *Rev. Mod. Phys.*, 85:1143–1189, 2013.

[62] P. Saramito. *Méthodes numériques en fluides complexes : théorie et algorithmes*. CNRS-CCSD, 2012. `http://cel.archives-ouvertes.fr/cel-00673816`.

[63] B. Halphen and Q.S. NGuyen. Sur les matériaux standards généralisés. *J. Méca.*, 14:39–63, 1975.

[64] G.A. Maugin. *The thermomechanics of plasticity and fracture*. Cambridge, 1992.

[65] B. Halphen and Q. S. Nguyen. Sur les matériaux standard généralisés. *J. Méca.*, 14:39–63, 1975.

[66] I. Cheddadi, P. Saramito, and F. Graner. Stationary Couette flows of elastoviscoplastic fluids are non-unique. *J. Rheol.*, 56(1):213–239, 2012.

[67] I. Cheddadi and P. Saramito. A new operator splitting algorithm for elastoviscoplastic flow problems. *Preprint*, 2013. `http://hal.archives-ouvertes.fr/hal-00809802`.

[68] Pierre Saramito. A new constitutive equation for elastoviscoplastic fluid flows. *J. Non-Newt. Fluid Mech*, 145:1–14, 2007.

[69] Pierre Saramito. A new elastoviscoplastic model based on the herschel-bulkley viscoplastic model. *J. Non-Newt. Fluid Mech*, 158:154–161, 2009.

[70] S. Bénito. *Modélisation et simulation du comportement mécanique des milieux plastiques mous : mousses liquides et émulsions*. PhD thesis, Université Bordeaux 1, Bordeaux, France, 2009.

[71] I. Cheddadi. *Modélisation numérique d'écoulements de mousse*. PhD thesis, Université Joseph-Fourier - Grenoble I, Grenoble, France, 2010.

[72] J. G. Oldroyd. On the formulation of rheological equations of states. *Proc. Roy. Soc. London A*, 200:523–541, 1950.

[73] D. D. Joseph. *Fluid dynamics of viscoelastic liquids*. Springer, 1990.

[74] Patrick Oswald. *Rheophysics: The Deformation and Flow of Matter*. Cambridge University Press, 2009.

[75] E. Rouhaud, B. Panicaud, and R. Kerner. Canonical frame-indifferent transport operators with the four-dimensional formalism of differential geometry. *Computational Materials Science*, 77:120–130, 2013.

[76] Olivier Cochet-Escartin, Jonas Ranft, Pascal Silberzan, and Philippe Marcq. Border forces and friction control epithelial closure dynamics. *Preprint*, 2013.

[77] Eva-Maria Schoetz, Marcos Lanio, Jared A. Talbot, and M. Lisa Manning. Glassy dynamics in three-dimensional embryonic tissues. *Preprint, arXiv:1307.4454*, 2013.

[78] Kenechukwu David Nnetu, Melanie Knorr, Josef Käs, and Mareike Zink. The impact of jamming on boundaries of collectively moving weak-interacting cells. *New J. Phys.*, 14:115012, 2013.

[79] Dapeng Bi, J. H. Lopez, J. M. Schwarz, and M. Lisa Manning. Energy barriers govern glassy dynamics in tissues. *Preprint, arXiv:1308.3891*, 2013.

[80] F. Graner, B. Dollet, C. Raufaste, and P. Marmottant. Discrete rearranging disordered patterns, part i: Robust statistical tools in two or three dimensions. *Eur. Phys. J. E*, 25:349–369, 2008.

[81] Philippe Marmottant and François Graner. Plastic and viscous dissipations in foams: cross-over from low to high shear rates. *Soft Matter*, 9:9602–9607, 2013.

[82] Alberto Puliafito, Lars Hufnagel, Pierre Neveu, Sebastian Streichan, Alex Sigal, D. Kuchnir Fygenson, and Boris I Shraiman. Collective and single cell behavior in epithelial contact inhibition. *Proc Natl Acad Sci U S A*, 109:739–744, 2012.

[83] Thomas Bittig, Ortrud Wartlick, Anna Kicheva, Marcos González-Gaitán, and Frank Jülicher. Dynamics of anisotropic tissue growth. *New J. Phys.*, 11:063001, 2008.

[84] T. Bittig, O. Wartlick, M. González-Gaitán, and F. Jülicher. Quantification of growth asymmetries in developing epithelia. *Eur Phys J E*, 30:93–99, 2009.

[85] T.A. McMahon. *Muscles, Reflexes, and Locomotion*. Princeton University Press, Princeton, 1984.

[86] Jocelyn Étienne, Atef Asnacios, Démosthène Mitrossilis, Valentina Peschetola, and Claude Verdier. How the cell got its shape : A visco-elasto-active model of the cytoskeleton. In *20e Congrès Français de Mécanique, 28 août/2 sept. 2011*, 25044 Besançon, France(FR), 2011. AFM, Maison de la Mécanique, 39/41 rue Louis Blanc, 92400 Courbevoie, France(FR).

[87] J. Étienne, D. Mitrossilis, J. Fouchard, N. Bufi, P. Durand, and A. Asnacios. The cell as a liquid motor: intrinsic mechanosensitive properties of the actomyosin cortex. *Preprint*, 2013.

[88] Justin S. Bois, Frank Jülicher, and Stephan W. Grill. Pattern formation in active fluids. *Phys. Rev. Lett.*, 106:028103, 2011.

[89] P. Marcq. Spatio-temporal dynamics of an active, polar, viscoelastic ring. *Preprint*, 2013.

[90] A. M. Sonnet and E. G. Virga. Dynamics of dissipative ordered fluids. *Phys Rev E Stat Nonlin Soft Matter Phys*, 64:031705, 2001.

[91] A. M. Sonnet, P. L. Maffettone, and E. G. Virga. Continuum theory for nematic liquid crystals with tensorial order. *J. Non-Newton. Fluid Mech.*, 119:51–59, 2004.

[92] P. Marmottant, C. Raufaste, and F. Graner. Discrete rearranging disordered patterns, part ii: 2d plasticity, elasticity and flow of a foam. *Eur. Phys. J. E*, 25:371–384, 2008.

[93] Guy B Blanchard, Alexandre J Kabla, Nora L Schultz, Lucy C Butler, Benedicte Sanson, Nicole Gorfinkiel, L. Mahadevan, and Richard J Adams. Tissue tectonics: morphogenetic strain rates, cell shape change and intercalation. *Nat Methods*, 6:458 – 464, 2009.

[94] L. C. Butler, G. B. Blanchard, A. J. Kabla, N. J. Lawrence, D. P. Welchman, L. Mahadevan, R. J. Adams, and B. Sanson. Cell shape changes indicate a role for extrinsic tensile forces in drosophila germ-band extension. *Nat. Cell Biol*, 11:859 – 864, 2006.

[95] Richard Kennaway, Enrico Coen, Amelia Green, and Andrew Bangham. Generation of diverse biological forms through combinatorial interactions between tissue polarity and growth. *PLoS Comput Biol*, 7:e1002071, 2011.

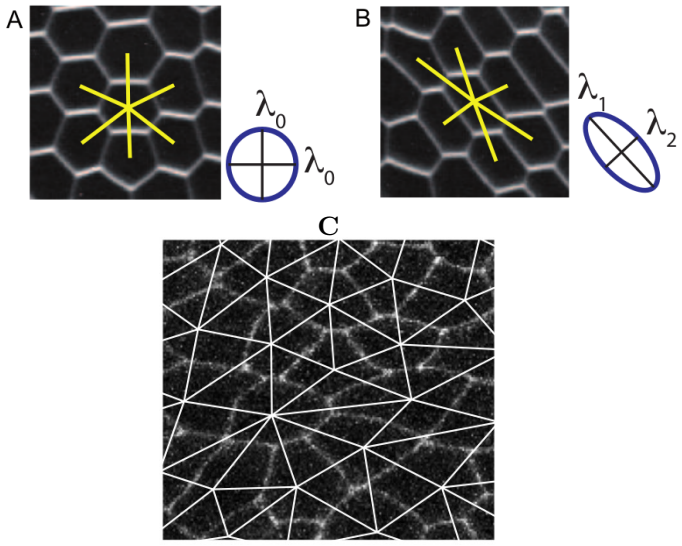

FIG. 11: Measurement of texture. (A) Snapshot of a foam, in an isotropic region; its texture has two equal eigenvalues. (B) Same foam, in an anisotropic region; ; its texture has two different eigenvalues. (C) A tissue. Straight lines, called "links", are drawn between centers of neighbouring cells. Reprinted from [80].

Appendix

APPENDIX A: TENSORIAL TOOLS TO DESCRIBE CELLULAR MATERIALS

The deformation and the deformation rate are among the most fundamental variables in the classical theory of continuum materials. In the case of cellular materials, the continuum description has to include the cell shapes, the neighbour configuration and other local geometrical properties. Blanchard *et* al. [93, 94] measure separately the deformation rate and the cell shape changes. Their difference is attributed only to the net effect of cell rearrangements, which is thus indirectly estimated.

Alternatively, Graner *et* al. introduce a direct and independent measurement of the deformation rate, the cell shape changes and the rate of intercalation, without any *a priori* assumption regarding the causal relationship between these quantities. This method, explained in detail in Ref. [80], has been applied to foams [92] and to tissues [16]. We recall it here briefly in the 2D case.

Consider two cells which share an edge (Fig. 11). Their centers of mass have coordinates $\vec{r}_1 = (x_1, y_1)$ and $\vec{r}_2 = (x_2, y_2)$. A pair of such cells is called a "link", characterised by the vector $\vec{\ell} = \vec{r}_2 - \vec{r}_1$ with coordinates $(X, Y) = (x_2 - x_1, y_2 - y_1)$. The link vector carries the information on link length and angle. The link matrix $\overline{\overline{\mathbf{m}}}$ is defined as:

$$\overline{\overline{\mathbf{m}}} = \begin{pmatrix} X^2 & XY \\ YX & Y^2 \end{pmatrix} \tag{A1}$$

It retains the information of link size and angle, but not of its sign. Averaging it over a group of cells, at any chosen length scale, reduces the whole cell pattern to the information of deformation and anisotropy over the corresponding set of links, called its texture, $\overline{\overline{\mathbf{M}}} = \langle \overline{\overline{\mathbf{m}}} \rangle$:

$$2D: \qquad \overline{\overline{\mathbf{M}}} = \begin{pmatrix} \langle X^2 \rangle & \langle XY \rangle \\ \langle YX \rangle & \langle Y^2 \rangle \end{pmatrix} \tag{A2}$$

There exist two orthogonal axes (eigenvectors) in which $\overline{\overline{\mathbf{M}}}$ would be diagonal, with strictly positive eigenvalues λ_i ($i = 1$ or 2). If we call $\langle \ell_+ \rangle$ the r.m.s. length of links in the direction of elongation (say, 1) and $\langle \ell_- \rangle$ the r.m.s. length of links in the direction of compression (say, 2), then $\lambda_1 \approx \langle \ell_+^2 \rangle / 2$ and $\lambda_2 \approx \langle \ell_-^2 \rangle / 2$. In 2D, $\overline{\overline{\mathbf{M}}}$ is represented by an ellipse with axes proportional to the eigenvalues λ_i. It is more circular in Fig. 11A than in Fig. 11B. This measurement easily becomes multi-scale upon coarse-graining over some spatial domain, by performing averages over links (lines in Fig. 11C); time averages over several images can be performed too.

The above mentioned kinematic tensors (the deformation rate, the cell shape changes and the rate of intercalation) can be expressed using the formalism based on this texture [80]. The cell shape changes correspond to the changes in texture. The links which appear (or disappear) in the time interval between two successive images of a movie characterise all changes in the cell pattern topology. All links which are conserved during the time interval between two successive images of a movie can be tracked: their changes express the relative motion of two neighboring cells, and thus measure the velocity gradient.

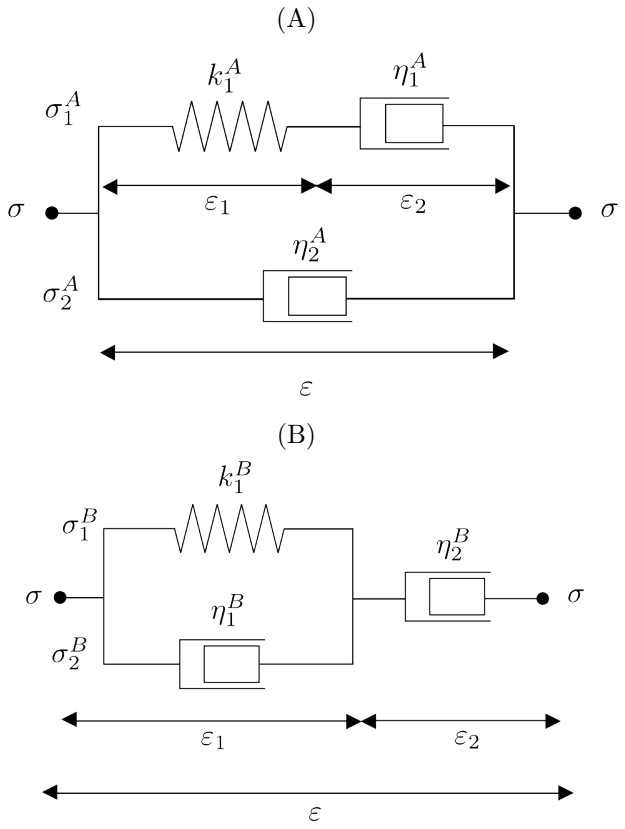

FIG. 12: Two rheological models with identical constitutive equation, Eq. (B1). (A) Maxwell-based model, same as Fig 1. (B) Voigt-based model.

APPENDIX B: NON-UNICITY OF THE DIAGRAM REPRESENTATION

Usually, when constructing a rheological diagram, one starts from physical insights about the material; for instance, in the case of a tissue: "cells store elasticity" or "cell rearrangements are negligible". Depending on the system configuration and structure, the corresponding forces and displacements are put in series or in parallel. If the component elements (*e.g.* springs or dashpots) are intuitively associated with precise cellular structures, then the topologies of these diagrams reflect how these structures are thought to be mutually connected mechanically.

Once the diagram has been constructed, a unique set of equations can be written (see Section II B 1). It contains the relevant parameters which can eventually be extracted from rheological data. If the model successfully reproduces the data, one is tempted to infer that the initial physical modelling has been correct and that the rheological diagram is validated. We now point out on a very simple example that *different rheological diagrams* may be associated to the *same equations*.

Fig. 12a, identical to Fig 1, shows a Maxwell element (linear viscoelastic liquid) in *parallel* with a dashpot. As shown in Section II B 1, the corresponding equation is of the form:

$$\dot{\sigma} + \alpha\sigma = \beta\dot{\varepsilon} + \gamma\ddot{\varepsilon} \tag{B1}$$

with

$$\begin{aligned} \alpha &= \frac{k_1^A}{\eta_1^A} \\ \beta &= \frac{\eta_1^A + \eta_2^A}{\eta_1^A} k_1^A \\ \gamma &= \eta_2^A \end{aligned} \tag{B2}$$

It happens that this equation also corresponds to a distinct rheological diagram, namely a Voigt element (linear viscoelastic solid) in *series* with a dashpot (Fig. 12b). In

the latter case the equation parameters are

$$\begin{aligned} \alpha &= \frac{k_1^B}{\eta_1^B + \eta_2^B} \\ \beta &= \frac{\eta_2^B}{\eta_1^B + \eta_2^B}\, k_1^B \\ \gamma &= \frac{\eta_1^B \eta_2^B}{\eta_1^B + \eta_2^B} \end{aligned} \tag{B3}$$

They can be obtained from those of Fig. 12a using:

$$k_1^B = k_1^A \frac{(\eta_1^A + \eta_1^A)^2}{(\eta_1^A)^2} \tag{B4}$$

$$\eta_1^B = \frac{\eta_2^A}{\eta_1^A}(\eta_1^A + \eta_1^A) \tag{B5}$$

$$\eta_2^B = \eta_1^A + \eta_1^A \tag{B6}$$

Conversely, the parameters for Fig. 12a can be obtained from those of Fig. 12b using:

$$k_1^A = k_1^B \frac{(\eta_2^B)^2}{(\eta_1^B + \eta_1^B)^2} \tag{B7}$$

$$\eta_1^A = \frac{(\eta_2^B)^2}{\eta_1^B + \eta_1^B} \tag{B8}$$

$$\eta_2^A = \frac{\eta_1^B \eta_2^B}{\eta_1^B + \eta_1^B} \tag{B9}$$

APPENDIX C: SCALAR, POLAR, AXIAL, TENSOR

In terms of symmetry, in 1D the main distinction is between variables which either change or do not change sign under the transformation $x \to -x$. In two or more dimensions, each parameter or variable used to describe the mechanical behaviour of a material can be classified according to its number of independent components: scalar, vector and tensor. To avoid ambiguities regarding vectors sometimes found in the literature, Ref. [95] suggests to distinguish polar and axial quantities We present here in 2D the vocabulary we use, which can be immediately generalised to 3D.

a. Scalar A scalar is simply a real number: it has a magnitude that can be ordered on a single scale. This is the case for the cell density ρ or for the concentration c.

b. Polar A vector consists in several components; for instance a magnitude and one (in 2D) or two (in 3D) angles. It is a polar quantity $\vec{p}$: its sign is significant, and changing $\vec{x} \to -\vec{x}$ transforms $\vec{p}$ in $-\vec{p}$. It is used to describe a force or a velocity, or a protein concentration whose distribution along a cell contour has a local maximum. It is usually represented graphically as an arrow.

A unit vector has only angles, and no information for magnitude: for instance the orientation of a polar molecule, or the direction of polarisation of a migrating cell.

c. Axial An axial quantity is unchanged under the transformation $\vec{x} \to -\vec{x}$ and its sign is not significant. It has a magnitude. Its angles are defined so as to identify opposite directions: in 2D, for instance, the angle is defined modulo π, *i.e.* between 0 and π. It describes the axis of a fiber, a nematic molecule, or a protein concentration whose distribution along a cell contour has two diametrically opposed maxima. It is often represented graphically as a bar (without any arrow) or as a bivector (a bar with an arrow at each end) whose length encodes the magnitude.

d. Symmetric tensor A symmetric tensor is usually represented graphically as an ellipse. It has two or three perpendicular axes in 2D or in 3D, respectively. It has one magnitude per axis. In 2D, one angle between 0 and π is enough to describe the orientation of both axes. A symmetric tensor remains unchanged under the transformation $\vec{x} \to -\vec{x}$. The adjective "symmetric" denotes the symmetry of components. Examples include the stress (magnitude is positive for traction, negative for compression), the deformation, the deformation rate, the inertia tensor.

The isotropic part of a symmetric tensor is its trace times the identity tensor. The information it conveys thus reduces to the trace, which is a scalar. The anisotropic part of a symmetric tensor, *i.e.* what remains when its symmetric part has been removed, is called the deviator: the sum of its (two or three) magnitudes is zero. In 2D, the information it carries reduces to one magnitude and one angle. It can be represented as a bar (usually oriented by convention along the axis with a positive magnitude).

A very different example is a tensor like the inertia of a fiber or a nematic molecule. It has one finite magnitude, the other(s) being equal to zero, and can be plotted as a bar whose length encodes the magnitude, like an axial quantity. Axial quantities can thus be considered as a subcategory of symmetric tensors.

e. General tensor Tensors which are not symmetric are characterised by a general matrix, *i.e.* four independent numbers in 2D. One example is the velocity gradient. In the case of the velocity gradient tensor one often separates its antisymmetric part, called the vorticity (represented, in 2D, as if it were a scalar) from the symmetric part, the deformation rate (represented as a symmetric tensor).

f. Pseudo-scalar, pseudo-vector The vorticity has its sign reversed under the transformation $\vec{x} \to -\vec{x}$. It is therefore considered as a pseudo-scalar (in 2D) or a pseudo-vector (in 3D). Incorporating vorticity (or any other pseudo-scalar or pseudo-vector such as a cross vector product) into equations is often easier in the form of the equivalent antisymmetric tensor (recall that vorticity can be seen as the antisymmetric part of the velocity gradient).

g. Higher order tensor Higher order tensors are often used to relate two usual (second order) tensors. For

instance, the elastic modulus relates the stress to the deformation in the linear response limit, and is intrinsically a fourth order tensor. However, for an isotropic material, such a fourth order tensor reduces to only a few independent coefficients. For instance, in linear elasticity, the relation between the stress and the deformation (two symmetric tensors) reduces to one linear scalar relation between the traces of both tensors and one proportionality relation between the deviators of both tensors. It is thus not necessary to use a fourth order tensor in that case. All other cases treated in the present article can also be expressed in simpler terms. Correspondingly, such higher order tensors are not discussed.

APPENDIX D: TRANSPORT OF ELASTIC DEFORMATION

The evolution of a tensor representing a quantity attached to the material, such as the elastic deformation $\bar{\bar{\mathbf{e}}}$, results not only from the physical ingredients (such as growth, plasticity, contractility, see Section III), but also from the transport by the velocity field. We here investigate in detail the latter contribution. We will see that it complements the $\vec{v}\cdot\nabla$ contribution that is used for scalars and vectors.

For simplicity, the coordinate system used to express the tensor is usually a fixed (orthonormal) referential. Meanwhile, the material is transported by the velocity field and the natural coordinate system used to describe the tensor is thus altered (and may be no longer orthonormal). For instance, if the material is rotated as a solid, the tensor rotates in the same manner. This implies that the time evolution of tensors, the so-called "objective derivative", involves new terms that are of order 1 in the elastic deformation [62, 72–74].

As discussed in Section II C, we have in mind a tissue that may undergo a large number of cell rearrangements (this is often realistic since cell shapes can deform only up to a finite limit) so that eventually the accumulation of rearrangements can constitute a large contribution to the total deformation ε. In Appendix D 1, we define elongation tensors and determine their time evolution. In Appendix D 2, we discuss their relation to deformation. In Appendix D 3, we derive the evolution equation for the deformation tensor. Finally, in Appendix D 4, we discuss volume conservation.

1. Elastic elongation tensors

A reasonable way to define the current elastic (tensorial) deformation $\bar{\bar{\mathbf{e}}}$ of a material is to quantify how much the current material state locally departs from a (local) relaxed state that would be obtained by cutting out a small region of interest [19]. This has recently been done in two different ways [53, 80] and applied to bubbles (or droplets) in the context of liquid foams (or emulsions, respectively). In both methods, the deformation $\bar{\bar{\mathbf{e}}}$ is assessed by *(i)* taking representative vectors $\vec{\boldsymbol{\ell}}$ attached to the material in its current configuration, *(ii)* determining how they differ from their original value $\vec{\boldsymbol{\ell}}_0$ and *(iii)* finding the deformation tensor $\bar{\bar{\mathbf{e}}}$ that is compatible with the change from $\vec{\boldsymbol{\ell}}_0$ to $\vec{\boldsymbol{\ell}}$. Rather than dealing with deformation $\bar{\bar{\mathbf{e}}}$ whose rest value is zero, both methods deal with (squared) elongation tensors, whose rest values are proportional to identity.

The method of Ref. [80] is operational on images (or movies) of 2D foams, as described in Appendix A. It measures only vectors $\vec{\boldsymbol{\ell}}$ in the current configuration. It relies on the assumption that the corresponding relaxed vectors $\vec{\boldsymbol{\ell}}_0$ (from bubble center to bubble center) are distributed isotropically with, say, a mean squared length $\langle\vec{\boldsymbol{\ell}}_0^T\vec{\boldsymbol{\ell}}_0\rangle = R^2$. It then provides the tensor $\bar{\bar{\mathbf{M}}} = \langle\vec{\boldsymbol{\ell}}\otimes\vec{\boldsymbol{\ell}}\rangle = \langle\vec{\boldsymbol{\ell}}\vec{\boldsymbol{\ell}}^T\rangle$ suitably averaged spatially. Thus $\bar{\bar{\mathbf{M}}} = R^2\,\bar{\bar{\mathbf{I}}}$ when the material is at rest.

The method of Ref. [53] starts with vectors $\vec{\boldsymbol{\ell}}_0$ located on a circle in the relaxed configuration ($\vec{\boldsymbol{\ell}}_0^T\vec{\boldsymbol{\ell}}_0 = R^2$) and on an ellipse in the current configuration ($\vec{\boldsymbol{\ell}}^T\bar{\bar{\mathbf{B}}}^{-1}\vec{\boldsymbol{\ell}} = R^2$), thus with $\bar{\bar{\mathbf{B}}} = \bar{\bar{\mathbf{I}}}$ when the current configuration is relaxed. This method is mainly a theoretical one, since the corresponding actual experiments require ablation, which is a destructive technique [19].

Let us now examine how the tensor $\bar{\bar{\mathbf{M}}}$ of the former method and the tensor $\bar{\bar{\mathbf{B}}}$ of the latter method evolve when the material is subjected to a velocity field $\vec{v}(\vec{r})$. After a time $\mathrm{d}t$ has elapsed, a vector $\vec{\boldsymbol{\ell}}$ attached to the material is turned into $\vec{\boldsymbol{\ell}}' = (\bar{\bar{\mathbf{I}}}+\bar{\bar{\xi}})\vec{\boldsymbol{\ell}}$, where we have noted $\bar{\bar{\xi}} \equiv \nabla\vec{v}\,\mathrm{d}t$. The new value of $\bar{\bar{\mathbf{m}}} = \vec{\boldsymbol{\ell}}\vec{\boldsymbol{\ell}}^T$ is $\bar{\bar{\mathbf{m}}}' = (\bar{\bar{\mathbf{I}}}+\bar{\bar{\xi}})\,\bar{\bar{\mathbf{m}}}\,(\bar{\bar{\mathbf{I}}}+\bar{\bar{\xi}}^T)$. Thus, $\bar{\bar{\mathbf{m}}}' - \bar{\bar{\mathbf{m}}} = \bar{\bar{\xi}}\bar{\bar{\mathbf{m}}} + \bar{\bar{\mathbf{m}}}\bar{\bar{\xi}}^T + \mathcal{O}(\bar{\bar{\xi}}^2)$. Averaging over center-to-center vectors $\vec{\boldsymbol{\ell}}$ yields: $\bar{\bar{\mathbf{M}}}' - \bar{\bar{\mathbf{M}}} = \bar{\bar{\xi}}\bar{\bar{\mathbf{M}}} + \bar{\bar{\mathbf{M}}}\bar{\bar{\xi}}^T + \mathcal{O}(\bar{\bar{\xi}}^2)$. Dividing by $\mathrm{d}t$ and taking the limit $\mathrm{d}t\to 0$ yields the time-derivative of $\bar{\bar{\mathbf{M}}}$:

$$\left(\frac{\partial}{\partial t} + \vec{v}\cdot\nabla\right)\bar{\bar{\mathbf{M}}} = \nabla\vec{v}\bar{\bar{\mathbf{M}}} + \bar{\bar{\mathbf{M}}}\nabla\vec{v}^T \tag{D1}$$

Regarding the tensor $\bar{\bar{\mathbf{B}}}$ of Ref. [53], its value after $\mathrm{d}t$ obeys: $\vec{\boldsymbol{\ell}}'^T\bar{\bar{\mathbf{B}}}'^{-1}\vec{\boldsymbol{\ell}}' = R^2$ hence $\vec{\boldsymbol{\ell}}^T(\bar{\bar{\mathbf{I}}}+\bar{\bar{\xi}}^T)\bar{\bar{\mathbf{B}}}'^{-1}(\bar{\bar{\mathbf{I}}}+\bar{\bar{\xi}})\vec{\boldsymbol{\ell}} = \vec{\boldsymbol{\ell}}^T\bar{\bar{\mathbf{B}}}^{-1}\vec{\boldsymbol{\ell}}$. Since this applies for many independent values of vector $\vec{\boldsymbol{\ell}}$ (on an ellipse), the tensors themselves are equal: $(\bar{\bar{\mathbf{I}}}+\bar{\bar{\xi}}^T)\bar{\bar{\mathbf{B}}}'^{-1}(\bar{\bar{\mathbf{I}}}+\bar{\bar{\xi}}) = \bar{\bar{\mathbf{B}}}^{-1}$. Taking advantage of the fact that $\bar{\bar{\xi}}$ is small: $\bar{\bar{\mathbf{B}}}' = (\bar{\bar{\mathbf{I}}}+\bar{\bar{\xi}})\bar{\bar{\mathbf{B}}}(\bar{\bar{\mathbf{I}}}+\bar{\bar{\xi}}^T) + \mathcal{O}(\bar{\bar{\xi}}^2)$ and thus it turns out that $\bar{\bar{\mathbf{B}}}$ evolves in the same manner as $\bar{\bar{\mathbf{M}}}$:

$$\left(\frac{\partial}{\partial t} + \vec{v}\cdot\nabla\right)\bar{\bar{\mathbf{B}}} = \nabla\vec{v}\bar{\bar{\mathbf{B}}} + \bar{\bar{\mathbf{B}}}\nabla\vec{v}^T \tag{D2}$$

Let us now compare $\overline{\overline{\mathbf{M}}}$ and $\overline{\overline{\mathbf{B}}}$ in more detail. As mentioned above, when the tissue is at rest, one has $\overline{\overline{\mathbf{M}}}/R^2 = \overline{\overline{\mathbf{B}}} = \bar{\bar{\mathbf{I}}}$. Since R is a constant, Eqs. (D1) and (D2) show that $\overline{\overline{\mathbf{M}}}/R^2$ and $\overline{\overline{\mathbf{B}}}$ evolve identically. As a result, they are actually equal not only when the material is at rest, but also at all times:

$$\frac{\overline{\overline{\mathbf{M}}}}{R^2} = \overline{\overline{\mathbf{B}}} \tag{D3}$$

2. Expression of the elastic deformation tensor

In Appendix D 1, we have derived the evolution of the elongation $\overline{\overline{\mathbf{M}}}/R^2 = \overline{\overline{\mathbf{B}}}$. We will now determine its relation to deformation tensors and choose one particular definition of the deformation $\bar{\bar{\mathbf{e}}}$. Let us first assume that some symmetric tensor $\bar{\bar{\mathbf{e}}}$ provides the link, up to first order, between the initial and the current material vectors:

$$\vec{\boldsymbol{\ell}} = [\bar{\bar{\mathbf{I}}} + \bar{\bar{\mathbf{e}}} + \mathcal{O}(|\bar{\bar{\mathbf{e}}}|^2)]\vec{\boldsymbol{\ell}}_0. \tag{D4}$$

where $|\bar{\bar{\mathbf{e}}}|$ is the norm of tensor $\bar{\bar{\mathbf{e}}}$. It is always possible to choose $\bar{\bar{\mathbf{e}}}$ symmetric since the absolute orientation of the local initial state is arbitrary (see Ref. [53] for detail). Hence, $\overline{\overline{\mathbf{M}}} = \langle \vec{\boldsymbol{\ell}}\,\vec{\boldsymbol{\ell}}^{\,T} \rangle = [\bar{\bar{\mathbf{I}}} + \bar{\bar{\mathbf{e}}} + \mathcal{O}(|\bar{\bar{\mathbf{e}}}|^2)]\langle \vec{\boldsymbol{\ell}}_0\,\vec{\boldsymbol{\ell}}_0^{\,T} \rangle [\bar{\bar{\mathbf{I}}} + \bar{\bar{\mathbf{e}}} + \mathcal{O}(|\bar{\bar{\mathbf{e}}}|^2)]$. Recalling that $\langle \vec{\boldsymbol{\ell}}_0\,\vec{\boldsymbol{\ell}}_0^{\,T} \rangle = R^2$, this yields:

$$\overline{\overline{\mathbf{B}}} = \frac{\overline{\overline{\mathbf{M}}}}{R^2} = \bar{\bar{\mathbf{I}}} + 2\bar{\bar{\mathbf{e}}} + \mathcal{O}(|\bar{\bar{\mathbf{e}}}|^2) \tag{D5}$$

At small deformations, all deformation measures obey Eq. (D4). Ref. [53] chooses to define the deformation tensor $\bar{\bar{\mathbf{e}}}$ such that higher order terms are identically zero:

$$\bar{\bar{\mathbf{I}}} + 2\bar{\bar{\mathbf{e}}} \equiv \overline{\overline{\mathbf{B}}} \tag{D6}$$

3. Evolution of the elastic deformation tensor

Combining Eq. (D2) and (D6) yields :

$$\left(\frac{\partial}{\partial t} + \vec{v}\cdot\nabla\right)\bar{\bar{\mathbf{e}}} - \nabla\vec{v}\bar{\bar{\mathbf{e}}} - \bar{\bar{\mathbf{e}}}\nabla\vec{v}^{T} = \frac{\nabla\vec{v} + \nabla\vec{v}^{T}}{2} \tag{D7}$$

In the rheology literature, the left-hand side of this equation is known as the *upper-convected derivative* (Eq. (19)) of the deformation tensor $\bar{\bar{\mathbf{e}}}$. Other definitions of the deformation than Eq. (D6), with higher order terms, yield an evolution equation that differs from Eq. (D7), see *e.g.* Ref. [80].

4. Volume conservation

Following the analysis of Ref. [53], let us now discuss the conservation of volume in the various terms of the constitutive equation.

If β_i are the eigenvalues of $\overline{\overline{\mathbf{B}}}$, the ellipse (or ellipsoid) $\vec{\boldsymbol{\ell}}^{T}\overline{\overline{\mathbf{B}}}^{-1}\vec{\boldsymbol{\ell}} = R^2$ defined by $\overline{\overline{\mathbf{B}}}$ has half-axes $\sqrt{\beta_i}\,R$, to be compared to the radius R of the circle (or sphere) in the relaxed configuration ($\vec{\boldsymbol{\ell}}_0^{T}\vec{\boldsymbol{\ell}}_0 = R^2$). Hence, the volume of the ellipsoid is $\Omega = \prod_{i=1}^{d}\sqrt{\beta_i} = \sqrt{\det\overline{\overline{\mathbf{B}}}}$ times larger than that of the sphere, where d is the dimension (1, 2 or 3) of space. Thus, the ratio of both volumes changes with a rate given by:

$$\begin{aligned}\frac{\dot{\Omega}}{\Omega} &= \frac{1}{\sqrt{\det\overline{\overline{\mathbf{B}}}}}\frac{\mathrm{d}}{\mathrm{d}t}\left(\sqrt{\det\overline{\overline{\mathbf{B}}}}\right)\\ &= \frac{1}{2\det\overline{\overline{\mathbf{B}}}}\frac{\mathrm{d}}{\mathrm{d}t}\left(\det\overline{\overline{\mathbf{B}}}\right)\\ &= \frac{1}{2}\mathrm{Tr}\left(\overline{\overline{\mathbf{B}}}^{-1}\dot{\overline{\overline{\mathbf{B}}}}\right)\end{aligned} \tag{D8}$$

Injecting Eq. (91) for the time evolution of $\overline{\overline{\mathbf{B}}}$ into Eq. (D8) above, one obtains:

$$\begin{aligned}\mathrm{Tr}(\overline{\overline{\mathbf{D}}}) &= \frac{\dot{\Omega}}{\Omega} + \mathrm{Tr}\left(\overline{\overline{\mathbf{B}}}^{-1}\overline{\overline{\mathbf{D}}}_p\right)\\ &\quad + \mathrm{Tr}\left(\overline{\overline{\mathbf{B}}}^{-1}\overline{\overline{\mathbf{g}}}\right) + \mathrm{Tr}\left(\overline{\overline{\mathbf{B}}}^{-1}D_a\right)\end{aligned} \tag{D9}$$

Thus the actual rate of volume change $\nabla\cdot\vec{v} = \mathrm{Tr}(\overline{\overline{\mathbf{D}}})$ can be decomposed into several contributions: the contribution from the elastic stretching (term $\dot{\Omega}/\Omega$), the (usually small) plastic contribution from the rearrangements, see Eqs. (21) and (22), the contribution from the growth rate, see Eqs. (42) and (44), and that from the active deformation rate, see Eq. (53).

APPENDIX E: MEASURING THE DIVISION AND APOPTOSIS RATES

Section III B incorporates the apoptosis rate k_a and the division rate k_d into a continuum model. Here we define operationally how these quantities can be extracted from experimental movies.

If the tissue is disordered enough (that is, if cells are not totally synchronized and spatially correlated), time and space scales Δt and Δx can be chosen to count the number of divisions and apoptoses in each space-time box of size $\Delta x\Delta t$. Then the apoptosis rate is :

$$k_a \equiv \frac{1}{\Delta t}\,\frac{N_{\mathrm{apo}}\,(\Delta x, \Delta t)}{N\,(\Delta x)} \tag{E1}$$

where N_{apo} is the number of apoptoses in the space-time box $\Delta x\Delta t$, and N is the number of cells in space box Δx, assumed to be roughly constant if $N_{\mathrm{apo}}\,(\Delta x, \Delta t) \ll$

$N(\Delta x)$. Similarly the division rate is :

$$k_d \equiv \frac{1}{\Delta t} \frac{N_{\text{div}}(\Delta x, \Delta t)}{N(\Delta x)} \tag{E2}$$

These measured rates have a meaning in terms of continuum description if $\Delta x \Delta t$ is sufficiently large to have $N_{\text{apo}}, N_{\text{div}} \gg 1$. Microscopy movies of a tissue can give access to its division and apoptosis dynamics in time and space.

As a consequence, *if* the tissue dynamics is ergodic *and if* the division rate k_d is constant, k_d^{-1} measures an average of the cell cycle duration. The definitions of k_d ad k_a remain operational and valid even when either of these conditions is not met. If a cell apoptosis eventually results in its complete disappearance, the contribution of apoptosis to growth is $-k_a$, and at the tissue scale the growth rate is:

$$g = k_d - k_a \tag{E3}$$